Ujjwal Shrestha

Structure from Motion applied to movable bed scale models

Master's thesis in Hydropower Development
Supervisor: Nils Rüther
June 2019

Master's thesis

NTNU
Norwegian University of
Science and Technology

Ujjwal Shrestha

Structure from Motion applied to movable bed scale models

NTNU
Norwegian University of
Science and Technology

Abstract

Many spatial data collection methods are available for a physical hydraulic model study considering mobile bed sediment. Some of them are highly sophisticated and advanced, which provide high-quality results in a shorter time. But they come with high capital and logistical cost and requires special training for execution. Whereas, the conventional surveying methodology, which is simple and inexpensive, require plenty of time for the measurement and processing of the data, provides a very low-quality data in comparison. That is why the recent developments in 'Structure from Motion' (SfM) technique have made it a potential candidate for an inexpensive and efficient tool for measurement of bed morphology in physical hydraulic model studies.

SfM method allows to simultaneously determine both the parameters of the camera and the 3-D structure of a scene by combining 2-D images taken from multiple viewpoints. It can create a dense point cloud out of a set of overlapping images taken even by a budget-friendly digital camera or a smartphone and freely available SfM software. The SfM method has already been used as an alternative for topographic surveying to create high-resolution digital elevation models (DEM). Some researchers have also used it for measurement of bed morphology in laboratory experiments.

In this study initially a low-cost tool SfM was introduced and applied in movable bed scale models to illustrate the potential of SfM applications in physical hydraulic models. Then six different SfM tools were chosen for the study and were used to create 3-D models of a physical hydraulic model. The cross-sections from the 3-D output were compared with the manual cross-section measurements. From this comparison a commercial SfM tool 'Agisoft PhotoScan' was chosen for further application in hydraulic models.

Two hydraulic models, one river model without any hydraulic structures and another having headworks structure components were chosen for the study. Firstly, SfM tool 'Agisoft PhotoScan' was applied to study the bed evolution in a physical river model at high sediment transport. The volume change in a certain reach of the river was estimated. Also, the cross-sections were compared with manual measurements done through a conventional surveying technique using a theodolite and a level machine. The accuracy of the output was compared with the manual measurement of length, cross-sections and sediment volume. Lastly, it was used to study the overall performance of headworks and trace the sediments in a model containing complex flushing hydraulic structures. Also, the flushed volume in certain flow and flushing mechanism was estimated and compared with manual volume measurement of flushed sediments.

The results conclude that SfM technique, in particular, Agisoft PhotoScan can be used as an inexpensive and efficient alternative for bed morphology measurements in physical hydraulic models with higher accuracy.

Preface

This thesis is the final work of my master's degree in Hydropower Development at NTNU. The thesis accounts for 30 credits and is written over 5 months (Jan 2019 – June 2019). The thesis is written in collaboration with the Project SediPass – NTNU, funded by The Research Council of Norway (RCN) and supervised by Nils Rüther (Associate Professor, Department of Civil and Environmental Engineering, NTNU).

First, I would like to express my sincere gratitude to my main supervisor, Nils Rüther for providing me the possibility and ability to do this thesis with important feedbacks and useful discussions. Also, thanks to my co-supervisor, Sanat Kumar Karmacharya for the time, encouragement, valuable guidance and support.

I would also like to acknowledge with great appreciation to Hydro Lab, Kathmandu, Nepal for providing me help and support to conduct my experiments.

Finally, I would like to express my very profound gratitude to my family and friends for providing me with unfailing support and continuous encouragement throughout my years of study and through the process of researching and writing this thesis. This accomplishment would not have been possible without them.

Trondheim- June 25, 2019.
Ujjwal Shrestha

Table of Contents

List of Figures

List of Tables

List of Abbreviations (or Symbols)

3-D	Three-Dimensional
2-D	Two-Dimensional
SfM	Structure from Motion
DEM	Digital Elevation Model
PDF	Portable Document Format
GCP	Ground Control Point
SIFT	Scale Invariant Feature Transformation
RANSAC	Random Sample Consensus
RMSE	Root Mean Square Error
MVS	Multi View Stereo
CMVS	Clustering views for Multi-View Stereo
PMVS	Patch-based Multi-View Stereo
TLS	Terrestrial Laser Scanning
UAV	Unmanned Aerial Vehicle
GPS	Global Positioning System

1 Introduction

In the present era of a technological revolution in geoscience, various methodologies are available, over conventional ground surveying techniques, for creating a high-resolution digital elevation model (DEM) of a topography. The traditional surveying techniques are very simple and have a low logistical cost, but it requires plenty of time for data acquisition and processing. The topographic data prepared from traditional surveying is likely to be of low quality and have limited flexibility. Recently, airborne and terrestrial laser scanning technology (Lohani & Mason, 2001) is used to get high-quality topographic data in the form of 3-D point clouds in a shorter time. Creating a high-resolution DEM in a shorter time requires a high logistical cost and specialized user expertise. That's why a revolutionary technique 'Structure from Motion' (SfM) has made it one of the best alternatives for the preparation of detailed 3-D model in a shorter period as well as in a low logistical cost. The ability to extract high resolution and accurate spatial data using a normal consumer-grade digital camera appears truly remarkable and the possibilities of SfM appears to be limitless (Nyimbili, 2016). SfM technique uses 2-D images taken in an overlapping pattern acquired from multiple viewpoints to create a high-quality 3-D dense point cloud. Nowadays, SfM technique is widely used in the field of Engineering, land surveying, Forensics, Archeology, Real State, Film and Entertainment, sports etc.

The SfM method has been used as an alternative tool for topographic surveying to create high-resolution DEM. Some researchers have also used it for measurement of bed morphology in laboratory experiments. In this study, SfM method was used to study and create a dense point cloud from a set of photographs representing various stages of a short reach of a river. The experiment was conducted in various river models available in the hydraulic laboratory at Hydro Lab, Kathmandu, Nepal. The results from the SfM method was compared with actual measurements (cross-sections and volume) in the physical model done with a conventional surveying technique using a theodolite and a level machine. Also, the accuracy of the tool was checked by comparing with the manual measurement of length, cross-sections and sediment volume.

1.1 The objective of the study

In Hydro Lab, for measurement of cross-sections are done manually by measuring at selected cross-sections and the data is interpolated in between. This involves a minimum of 3 personnel and plenty of time and effort. However, it gives a very low dense data. Also, there might be various errors in measurements. Also, the volume calculation manually is a very tedious process. Thus, a non-intrusive alternative method "Structure from Motion (SfM)" could be a better and economical option to get a relatively accurate 3-D point cloud for Hydraulic laboratories.

The objective of the study was to introduce and apply this low-cost tool SfM in physical hydraulic models in Hydro lab and create 3-D models using SfM tools. Thus, compare the output with manual measurements (cross-section comparison, Volume comparison) and

1

check the accuracy of the output with the manual measurement of cross-section and sediment volume.

1.2   Problems and limitations

Due to the non-uniform lighting conditions in the physical models in the lab, it was very difficult to capture a set of images in the same manual camera setting, so a proper time of the day had to be chosen when the lighting conditions in the model was uniform. Also, the shadows and dark images needed to be avoided to get sharp and detailed photographs.

The study was limited to the model in a dry state containing no water. The study of the formation of bed morphologies, tracing the sediment transport and flushed volume of a physical model was done after completely draining water from the model.

For the models containing Hydraulic structures, the glossy and non-textured surface created some problems in image processing.

1.3   Outline of the thesis

The thesis layout follows all the processing stage of spatial data acquisition starting from GCP positioning, Image capturing, Image processing and ending with post-processing and results, discussion and conclusion.

Chapter 1 deals with the objective of the study and some introduction to the study.

Chapter 2 is based on the theory and literature of the study.

Chapter 3 describes the methodology of the study.

In Chapter 4, two different case studies and a cube box accuracy test are discussed.

Finally, Chapter 5 and Chapter 6 presents the results and conclusion.

2 General Theory

2.1   Photogrammetric heritage

In this decade automated aerial and close-range photogrammetry has become a powerful and widely used tool for three-dimensional topographic modeling (Fraser & Cronk, 2009; Remondino & El-Hakim, 2006). Structure from motion (SfM) has evolved from the machine vision community. It owes its existence to innovations developed many generations ago, particularly in photogrammetry. The idea used to establish the spatial relationship between images, the coplanarity condition, was applied in the 1950 and 1960s for numerical aerial triangulation and mapping from aerial photography (Thompson, 1965). The bundle adjustment was later established by (Duane, 1971; Granshaw, 1980; Kenefick, Gyer, & Harp, 1972). A perfect metric camera can only generate images which are distortion free. However, a self-calibrating bundle adjustment (Faig & Moniwa, 1973; Kenefick et al., 1972) is capable of modeling and estimating additional parameters suitable to represent a wide range of internal distortions associated with consumer-grade digital cameras. The freely available or commercial and fully automated software packages are flexible, and they can process the images taken from different camera models, each frame may, therefore, be calibrated individually.

SfM has been already used in various field of hydraulic engineering. Alan Karsprak used it to find the relationship between particle travel distance and channel morphology from physical models of braided rivers (Kasprak, Wheaton, Ashmore, Hensleigh, & Peirce, 2015). R. Zhang used it for generation and comparison of Terrestrial Laser Scanning (TLS) and SfM based 3-D models of solid shapes in hydromechanics research (Zhang, Schneider, & Strauß, 2016). Baptiste Marteau applied SfM to study geomorphic change resulting from river restoration actions (Marteau, Vericat, Gibbins, Batalla, & Green, 2017). Philipp Thumser applied this technique for the characterization of riverine systems in the headwaters of the Volga river (Thumser et al., 2017). Jacob A.Morgan applied SfM in laboratory flume study (Morgan, Brogan, & Nelson, 2017). Gonzalo Duró used this method for Bank erosion processes measured with UAV-SfM along complex bank lines of a straight mid-sized river reach (Duró, Crosato, Kleinhans, & Uijttewaal, 2018).

2.2 Structure from motion

Structure from motion is like stereoscopic photogrammetry in which a 3-D structure is developed from a series of overlapping 2-D images taken from multiple positions as shown
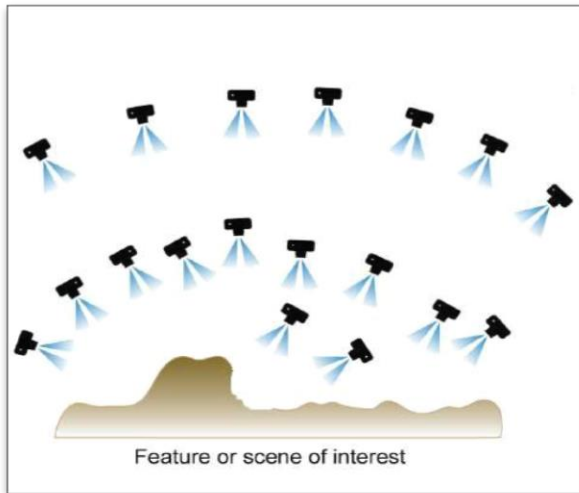
Figure 2-1 Image acquisition with sufficient overlap and from different position for Structure from motion Photogrammetry (N. Micheletti, 2015)
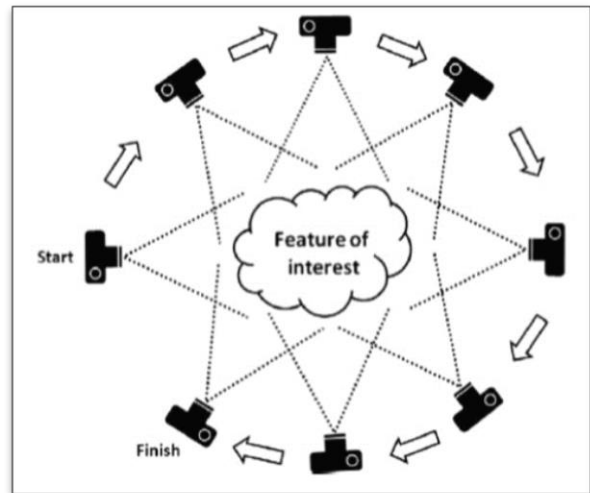
Figure 2-2 Multiple, overlapping photographs as input to feature extraction and 3-D reconstruction algorithms (Westoby, 2012)

in Figure 2-1 and Figure 2-2. Differing from the conventional photogrammetry, SfM method utilizes advanced algorithms by which it automatically solves the relative camera positions, orientation and geometry of the target object based on the features extracted from the set of overlapping images using a highly redundant iterative bundle adjustment procedure (Snavely, 2008). It results in a three-dimensional location of the feature point in the form of a sparse cloud in an arbitrary 3-D coordinate system. The sparse point cloud is then enhanced using Multi View Stereo (MVS) techniques (Furukawa, 2010). This technique has the capacity to generate very high-resolution point clouds removing the gross errors and develop a visually impressive 3-D model.

Furthermore, SfM uses a normal digital camera or a smartphone and a low cost or sometimes free software for processing. Also, some internet-based processing is available which enable us to upload images, process and download the 3-D data in minutes. Most SfM tools are now fully automated. Its advantage is that it provides us a black box tool where no expert supervision is necessary. (N. Micheletti, 2015)

2.3   Principle of SfM

The basic principle of SfM can be compared to a human eye. Humans perceive a three-dimensional structure of the surrounding by moving around it. Information is obtained from images sensed over time when the observer moves and the object around the observer move (Shapiro & Stockman, 2001).
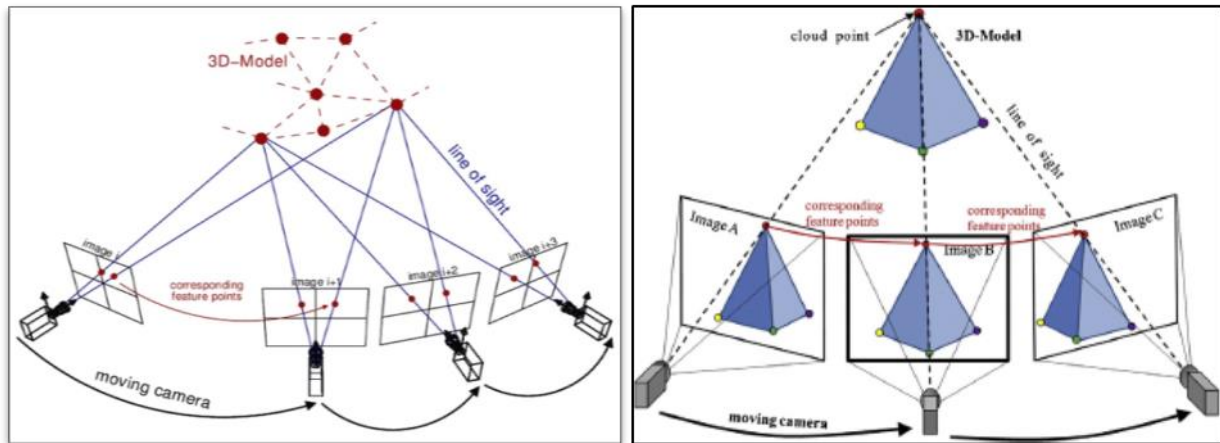
Figure 2-3 Photogrammetric principle (Theia-sfm.org, 2016; Yang, 2012).

SfM approach differs from traditional photogrammetry which requires 3-D location and angle of the camera(s), or the 3-D location of control points. The automatic identification of matching feature from multiple images in SfM creates the scene geometry, detecting camera angle and location automatically (Snavely, 2008). The camera positions estimated from SfM lacks the scale and orientation, thus the 3-D point cloud generated is in a relative coordinate system which can be converted to an absolute coordinate system through scaling, rotation, and translation (Westoby, 2012). It can be done by introducing several Ground Control Points (GCPs) with a known object-space-coordinates. The coordinates of GCPs can be obtained by ground survey either by GPS or manual survey via theodolite and level machine.

2.4   General workflow

There are various algorithms available for application of SfM, but the general workflow remains the same (Westoby, 2012) (James & Roboson, 2012) (C. N. Micheletti & Lane, 2015). Workflow diagram in Figure 2-4 describes the general workflow of Structure from Motion.
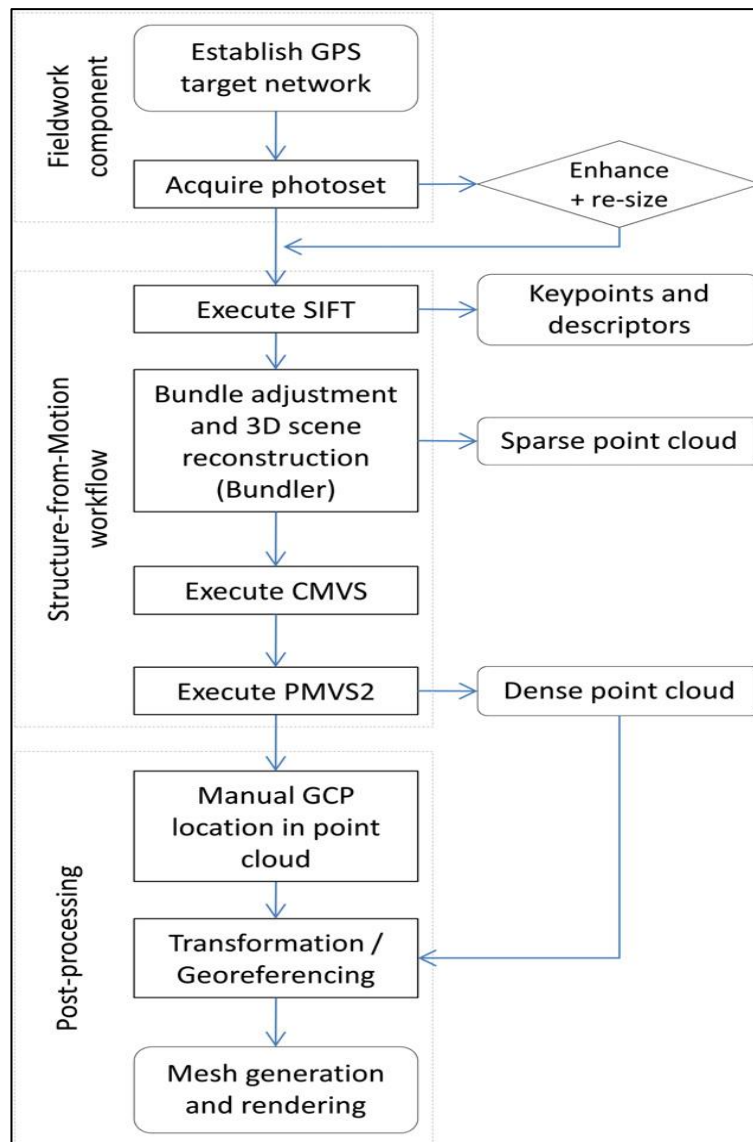
**Figure 2-4 Structure from Motion General Workflow
(Westoby, 2012)**

2.4.1 Image acquisition and keypoint extraction

From the multiple images taken from varying angles with enough overlap, the key features in each image are identified and a 3-D location of the feature is estimated using the Scale Invariant Feature Transformation (SIFT) object recognition system popularized by Snavely (2008). Overall scales and locations in each individual image, the feature of interest, or 'keypoints', are automatically identified and followed by the generation of a feature descriptor, computed by transforming local image gradients into a representation that is largely insensitive to variations in illumination and orientation (Lowe, 2004). This descriptors are solitary and allow features to be matched in large datasets. The number of key points in an image depends upon the image resolution and texture. Figure 2-4 shows the stages of keypoint selection. A close range shot images are sharper, dense and of high

resolution, which increases the spatial density of the final point cloud. Increasing the distance between camera and area of interest decreases the density of point cloud.

Depending upon the lighting conditions, complex features in individual scenes, the image texture is highly influenced, so it is difficult to set a minimum number of images necessary for successful scene reconstruction. However, a minimum of three images is required for corresponding features to be visible. Obtaining as many images as an input as possible considering given logistical constraints is recommended since it optimizes the ultimate number of key point matches and system redundancy. But a larger number of images does not necessarily mean better results (Westoby, 2012).
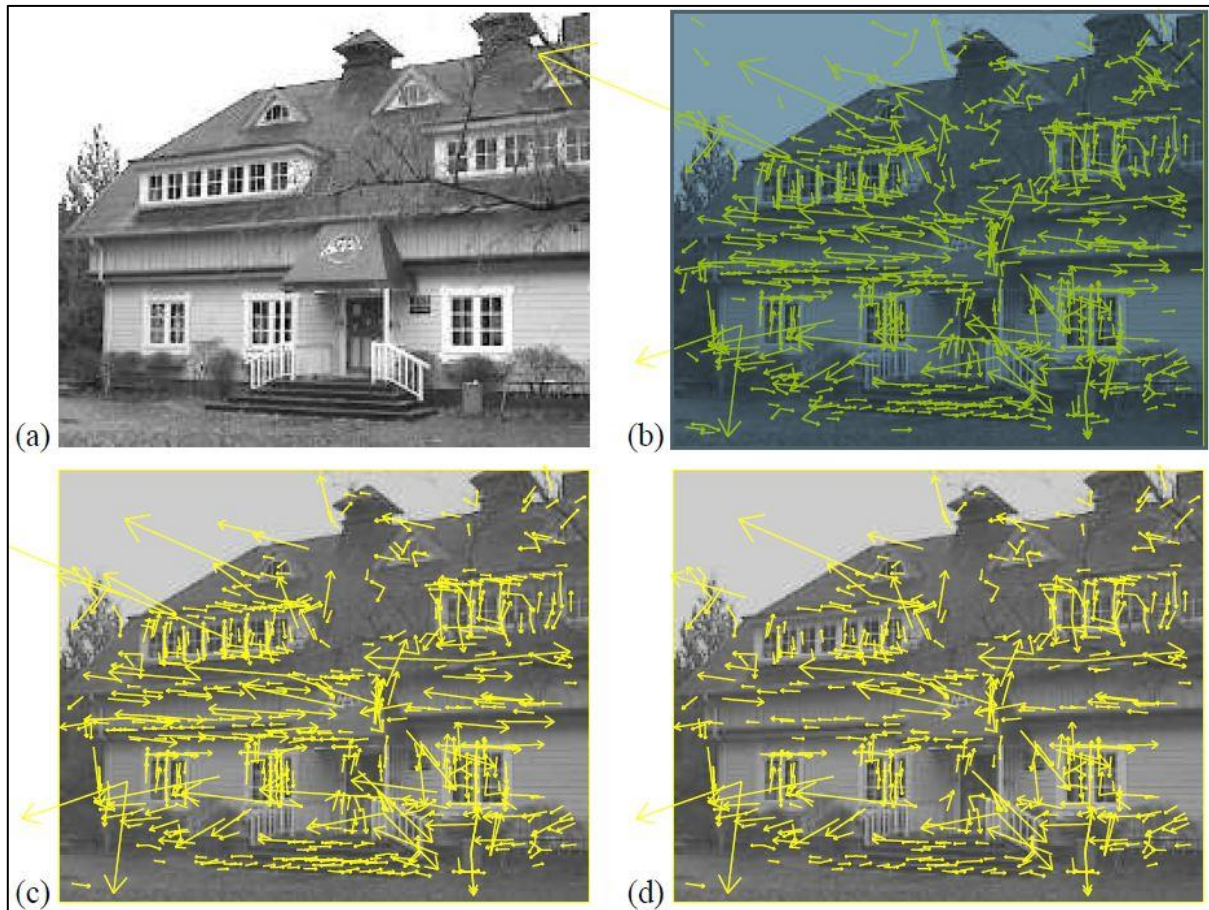
Figure 2-5 (a) The 233x189 pixel original image. (b) The initial 832 keypoints locations at maxima and minima of the difference-of Gaussian function. Keypoints are displayed as vectors indicating scale, orientation, and location. (c) After applying a threshold on minimum contrast, 729 keypoints remain. (d) The final 536 keypoints that remain following an additional threshold on ratio of principal curvatures.

2.4.2 3-D scene reconstruction

The sparse bundle adjustment (Snavely, 2008) is used to estimate camera angle and extract a low dense or sparse point cloud. As described by Arya (1998) and Fischler & Bolles (1981), using approximate nearest neighbor and Random Sample Consensus (RANSAC) algorithms, keypoints in multiple images are matched and tracks linking specific keypoints in a set of images are established. Tracks comprising of a minimum of three

images and two keypoints are used for point-cloud reconstruction, others failing these criteria are automatically abandoned (Sanvely, Seitz, & Szeliski, 2006). Using this method, unwanted features like people moving across the study area, non-static objects unintentionally captured in image set are automatically removed from the dataset before the 3-D reconstruction (Furukawa & Ponce, 2007).

The camera pose orientation is reconstructed using a similarity transformation. While, minimization of errors is achieved using a non-linear least-squares solution (Szeliski & Kang, 1994) (Nocedal & Wrighr, 1999). Now, the triangulation is used to estimate 3-D point positions and reconstruct the scene geometry. The fully automated process from key point extraction to a reconstruction of scene geometry is a distinct advantage of SfM over traditional photogrammetry.

2.4.3 Post-processing and DEM generation

The 3-D point cloud generated by the 3-D reconstruction process as described in 2.4.2 lacks the scale and orientation. Transformation of the relative coordinate to an absolute coordinate system can be done using rotation and translation matrix, and a scale factor discussed in 3.2. Various software involved in the processing of images and post-processing shall be discussed in 2.5. After the scaled 3-D point cloud is obtained, the point cloud can be decimated according to our necessity. Also, the mesh, texture, and DEM can be generated using the point cloud file. The point cloud files can be exported to a software 'Cloud Compare' to calculate volume changes in different hydraulic stages. Contour maps can be generated using point clouds and cross-section at any section of the model can be plotted.

2.5 Photogrammetry software

Due to the wide applications of SfM, nowadays there are various software available for its implementation. Following six software were selected for its application in the physical hydraulic models and the output was compared with manual measurements. The list of these six software and their processing capability, license and price are listed in Table 2-1. Among which first two are commercial software whereas the remaining four are free.

Also, a paper was written on these software comparisons, and presented at "International Symposium on Current Research in Hydropower Technologies" on 9th of April 2019, organized by Turbine Testing Lab, Kathmandu University, Dhulikhel, Nepal. (http://ttl.ku.edu.np/conference-proceedings/). See **Appendix 1** for the attached paper (on review).

The conclusion from the paper states, "The free and open source software are also capable of producing good results as compared to results from commercial software. Moreover, free and open sourced software offers more control to the users and hence have huge potential for researchers to produce even better-quality results. But for commercial purposes, where quality results are required in a shorter time with minimum involvement of the user, commercial software are recommended. For example, PhotoScan and ReCap can perform all the processes including scaling of the final model output and DEM generation within one platform and hence provide the complete solution. Whereas, free

and open sourced software requires additional third-party software to perform different processes e.g. Meshlab for geo-referencing the output model."

So, for further processing of images and post-processing, a commercial software 'Agisoft PhotoScan' was used.

Table 2-1 SfM software selected for study

Tools	Feature Extraction	Sparse reconstruction	Dense Reconstruction	Mesh Generation	Post Processing	Developer	License	Pricing USD	Remarks
PhotoScan (Metashape)					Texture and DEM	Agisoft LLC, Russia	Commercial	$3499 for pro and $179 for standard	
Autodesk ReCap					Texture	Autodesk Inc, USA	Commercial	$40 per month $305 per year $915 per 3year	Free academic license upto 100 images only.
Visual SfM			PMVS/CMVS	Meshlab	Meshlab	Changchang Wu	Free but not for commercial	-	
Regard3D					Texture	Roman Hiestand, Switzerland	Free and Open source	-	
Meshroom					Texture	Alice Vision	Free and Open source	-	Requires CUDA-enabled GPU with min computing capacity 2.0
COLMAP			MVS		Meshlab	Johannes L. Schonberger, Stwizerland	Free	-	For dense reconstruction and further, CUDA-enabled
MVS	Multi-View Stereo				MVS	Can be run in the same software environment			
PMVS	Patch-Based Multi-View Stereo				Meshlab	Results are exported to a different software for the tasks			
CMVS	Clustering views for Multi-View Stereo								

2.5.1 Agisoft PhotoScan

Agisoft PhotoScan (now available as Agisoft Metashape) is commercial software developed by Agisoft LLC, Research Company founded in 2006 in Russia. It is capable of processing both areal and close-range photographs. Agisoft PhotoScan is an advanced image-based 3-D modeling software which creates professional quality 3-D content from still images. Based on the recent MVS 3-D reconstruction technology it can process arbitrary images and is an efficient tool in both controlled and uncontrolled conditions. Images can be taken from any positions, considering that the object is visible on at least two images. Fully automated image alignment and 3-D model reconstruction is one of the features of it ("Agisoft," 2019). Throughout various case studies, Agisoft PhotoScan proves to produce quality and accurate results ("Agisoft," 2019).

It is easy to use software which offers all the capabilities from processing images to 3D model generation, orthomosaic and producing DEM. It also includes additional pre-processing and post-processing features like georeferencing and manual camera calibration. Professional edition of the software is priced USD 3,499 and the standard edition is available for USD 179 ("Agisoft," 2019). However, the standard edition itself is

enough for sthe generation of 3D models and lacks only other extra features that professional edition offers.

2.5.2 CloudCompare

CloudCompare is a 3-D point cloud and mesh processing open source software. It was created in a collaboration between 'Telecom ParisTech' and the R&D division of 'Électricité de France'. The CloudCompare project began in 2003 with the Ph.D. of Daniel Girardeau-Montaut on Change detection on 3-D geometric data (Girardeau-Montaut, Roux, Marc, & Thibault, 2005). It was originally designed to compare two dense 3D points clouds or between a point cloud and a triangular mesh. Now, it has been extended to a more generic point cloud processing software, including many advanced algorithms like registration, resampling, color/normal/scalar fields handling, statistics computation, sensor management, interactive or automatic segmentation, display enhancement, etc.("CloudCompare," 2019).

CloudCompare provides a set of basic tools for manually editing and rendering 3D points clouds and triangular meshes. It also offers various advanced processing algorithms, among which methods for performing volume difference computation is one of them. Two-point cloud files from a SfM tool PhotoScan can be exported to any file format (OBJ, PLY, STL, FBX, etc.) can be imported directly to CloudCompare. The point cloud files can be further edited or trimmed to match the two-point cloud files for computation of volume. The volume can be estimated using compute '2.5D volume' tool, selecting the grid size as required.

3 Methodology

3.1 Model General Characteristics

Physical scaled hydraulic models available in Hydro Lab Pvt. Ltd, Kathmandu Nepal were used for the study. Two hydraulic models in the lab were selected, one river model without any hydraulic structures and another having headworks structure components. Firstly, SfM tool 'PhotoScan' was applied to study the bed evolution in a physical river model at high sediment transport. Also, the volume change in a certain reach of the river was estimated using SfM tool. Lastly, SfM was used to study the overall performance of headworks and trace the sediments in a model containing complex flushing hydraulic structures. Also, the flushed volume in certain flow and flushing mechanism was estimated.

Figure 3-1 A river model without hydraulic structures (Photo: Hydro Lab)

3.2 Ground Control Points (GCP) and Georeferencing

A referenced model, be it a mesh or a DEM serves as a ground for length, area, volume, and profile measurement. In order to achieve 3-D output in an absolute coordinate system from a relative coordinate system, a pre-defined set of coordinated points generally known as Ground Control Points (GCP) are needed to be set in the physical model. They are manually identified in the point cloud and the computation of approximate transformation is done. Also, it is possible to get an absolute coordinated final product without placing manual markers, if the images from a GPS enabled camera is used for processing. However, the manual marker placement with a pre-defined coordinate system is usually more accurate allowing more precise geo-referencing. A rigid body transformation decomposed to a rotation and translation matrix is used for transforming the coordinates.

This transformation solution is described by (Horn, 1987) as absolute orientation using unit quaternions.

These GCPs should be distributed in such a way that it covers all the concerned area. A GCP should be visible in at least 3 images (Westoby, 2012). For a set of images taken from 20m above the ground in the area of $0.025km^2$, 10 nos. of GCPs were used to achieve Root mean square error (RMSE) to 0.04m (Goldstein, 2015). A minimum number of 5 GCP is also recommended by (N. Micheletti, 2015)

For higher accuracy in close range photogrammetry 13 to 19 GCPs were placed according to the physical model size. These GCPs were distributed such that they represented all the section of the river reach under survey. They should neither be too near to river bed since the deposition and scouring of sediments will disturb the GCPs location, nor too far from the interest area. Large and clear GCP marks were made, but still with thin lines, so that the exact center of the point is clear (Figure 3-2). Unique names i.e 'R' for right bank and 'L' for Left bank followed by a number or letter was given.
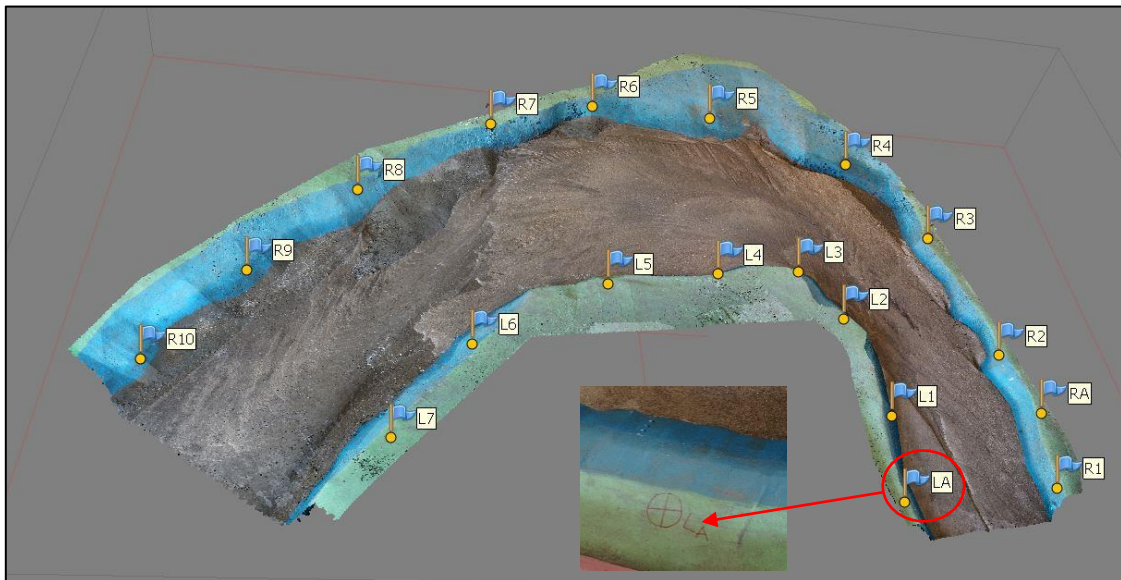
Figure 3-2 GCPs in a small reach (13m long) of river model (Model 1) in Hydro lab

The coordinates of GCPs were surveyed manually, in reference to three benchmarks established for the model, using a digital theodolite and a level machine using two angle measurement technique described in 3.5. GCPs should be visible from the benchmark points to get their precise location.

X, Y and Z coordinates obtained from manual survey was imported and placed to their respective places (described in 4.3.2). The Root Mean Square Error (RMSE) value was calculated to determine the accuracy of the GCPs. RMSE value quantifies how different a set of values are. The smaller an RMSE value, the closer predicted and observed values are. Formulas involved in the calculation of RMSE are presented below:

Error in X (Ex) = X-coordinate measured – X-coordinate estimated.

Error in Y (Ey) = Y-coordinate measured – Y-coordinate estimated.

Error in Z (Ez) = Z-coordinate measured – Z-coordinate estimated.

$$X_{RMSE} = \sqrt{\sum_{i=0}^{n}(Ex)^2 \big/ N} \ , \ Y_{RMSE} = \sqrt{\sum_{i=0}^{n}(Ey)^2 \big/ N} \ , \ Z_{RMSE} = \sqrt{\sum_{i=0}^{n}(Ez)^2 \big/ N}$$

$$RMSExyz = \sqrt{\left\{\sqrt{\sum_{i=0}^{n}(Ex)^2 \big/ N}\right\}^2 + \left\{\sqrt{\sum_{i=0}^{n}(Ey)^2 \big/ N}\right\}^2 + \left\{\sqrt{\sum_{i=0}^{n}(Ez)^2 \big/ N}\right\}^2}$$

Where N = number of GCPs

3.3   Image Acquisition

A random trial in a 20 m long physical model built in 1:40 scale was done to get an idea for image capturing. The recommended overlap for most cases is at least 75% frontal overlap (with respect to the flight direction) and at least 60% side overlap (between flying tracks), (PIX4D support, 2019). It is recommended to take images with a regular grid pattern as shown in Figure 3-3. However the random trial done in the physical model with a nonregular pattern also resulted in a considerable output.
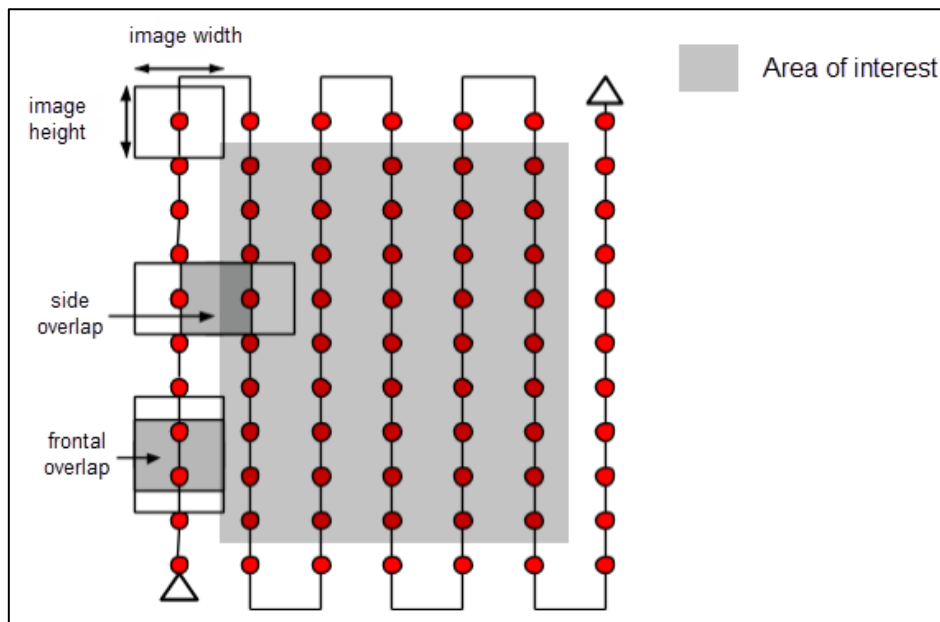
Figure 3-3 Ideal Image Acquisition Plan - General case (PIX4D support, 2019)

From the trials done with a different number of images taken for the same model, it was found that larger the number of images taken, the denser was the point cloud having more details. However, an excessive number of images led to larger processing time and heavier dense point cloud file. Medium dense cloud selection resulted in a sufficient amount of point cloud with considerable processing time and a reliable 3-D output.

13

Figure 3-4 Camera used for image acquisition

Sony α6300 (model ILCE-6300), mirrorless digital camera with 24-megapixel Exmor RS sensor and 425 phase detection autofocus points (Figure 3-4), was used to capture the images. The camera setting has a significant impact on output. From the trials, some important recommendations were found like, the manual mode in the camera setting is highly recommended over auto mode to ensure uniformity in camera parameters, the same setting for a set of images is necessary and zooming is not recommended. The 3-D output from the random trial is shown in Figure 3-5 and Figure 3-6.
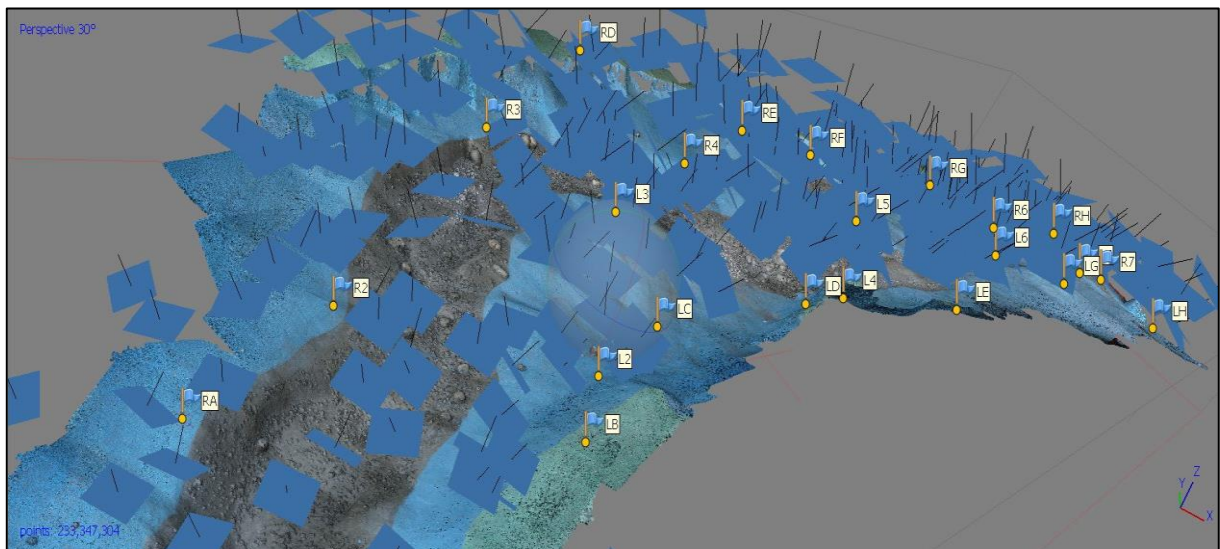
Figure 3-5 Images taken randomly covering all interest area in a non-grid pattern
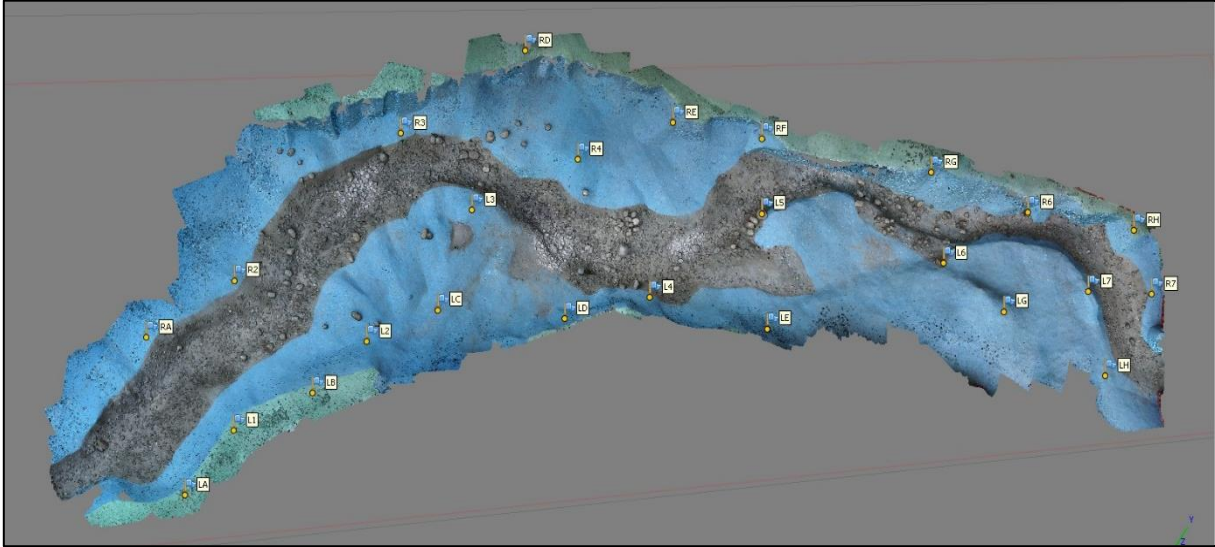
Figure 3-6 Final 3-D output from the trial

For the final output, the following camera settings were used:

- Shutter Priority (S) (Shutter speed is selected by the user, but ISO and aperture are auto-adjusted according to lighting conditions of the model)
- Shutter speed: 1/80 sec (For Hand shot 1/80 to 1/100 is recommended to get clear images)
- ISO<1000 (as less as possible to get sharp and detailed images, higher ISO produces grainier images)
- Aperture: F8 – F13 (in Shutter priority mode, the aperture is automatically adjusted according to model lighting conditions)
- Focal length: 16 mm (no zoom recommended)
- Image format: **JPEG** (shooting in raw format and saving as tiff is recommended for more detailed and better-quality images.

3.4 Image processing

There are various SfM software available to process the images, but the general principle remains the same as described in 2.4. Various freely available software like Visual SfM, Meshroom, Regard 3-D, COLMAP and commercial software like PhotoScan (now Metashape) and ReCap discussed in 2.5, were used in a physical hydraulic model to create a 3-D point cloud and the results were compared with the manual measurements (see **Appendix 1**).

From the comparison of various freely available and commercial software, PhotoScan was selected for further study because of its capability to perform all the processing including scaling and coordinate transformation by itself. Also, PhotoScan is capable of auto camera calibration feature in which it detects images taken from different cameras and divides them into calibration groups according to the image resolution or camera type or focal length. See **Appendix 2** for detail steps involved in image processing and scaling using PhotoScan.

The specifications of the workstation used for image processing was:

- Operating System: Microsoft Windows 7 Ultimate 64-bit
- Processor: Intel® Core™ i7-4790 CPU @3.60GHz
- Installed memory (RAM): 32 GB
- GPU: NVIDIA GeForce GTX 750 Ti -18 GB available memory

3.5 Field measurements

3.5.1 GCP coordinate calculation

Obtaining the accurate coordinates of the GCPs was important for the overall accuracy of the 3D model output. The horizontal angle to each GCP was measured placing a theodolite in one of the known benchmarks, followed by a distance measurement (measuring tape) from the benchmark to each of the GCPs. This method had a large degree of error. Mainly this was because of the difficulties in keeping the measuring tape straight, obstacles between benchmark. The measuring tape had to be held in the air for the measurement. A plumb bub was used for extending the point to the measuring tape. The measurement was read to the nearest millimeter. All these factors play a vital role in the accuracy of measurements, which had to be improved if a set of more accurate coordinates should be obtained.

Instead of making one angular and one distance measurement when calculating the X and Y coordinates of the GCPs, two angular measurements were used (see **Appendix 5** and **Appendix 6** for calculation sample). The location of the GCP was found using trigonometry. The known distance between the two benchmarks together with the two angles towards the GCP makes it possible to calculate its XY position. The theodolite used for the angular measurements, measures down to a thousandth of a gradient, making the calculations more accurate than with the previous method. The disadvantages of this method are that the GCPs must be visible from both benchmarks.

For the elevation assessment of the GCPs, the level machine and staff were used. The level machine was placed in a location where all GCP were visible, then the level at a benchmark was read and finally, the level at each GCP was taken (see Appendix 6 for Z coordinate calculation). It was a bit troublesome to manage the staff to the exact middle of the GCP point, the staff must be held exactly vertical and the measurement was read to the nearest millimeter.

3.5.2 Manual cross-section measurement

Cross-sections are very useful, as they can show what level of sediment has been disposited at different places, which is valuable information for the final review of the river model. The process of obtaining cross-section manually is quite tedious, needs many measurements, so demands more time and requires at least three people. The method has many sources of error. The measuring bar used in the process only shows down to a millimeter. Furthermore, the readings and set up of the equipment is relying on people, making error unavoidable. Figure 3-7 shows the manual cross-section measurement in a physical model.

Figure 3-7 Manual cross-section measurement (Hydro Lab)

Manually, the cross-sections were measured at different marked sections and later compared with the SfM cross-sections. For the measurement of the cross-section, a long scale bar is placed on the marked section in the same level lying either side of the model. The scale bar is equipped with adjustable staff which can move through the section horizontally. A level machine is placed in a visible position. Then, the reading is taken in each corresponding distance of the bar starting from the zero end. The number of points reading taken in each cross-section was 5 to 20, depending on the width of the interest area of the river reach. It took around 3 hours for 3 personnel to measure nine cross sections in a model and for data entry and cross-section plot more than one and a half working days were spent.

4 Case Study

4.1 Cube box test

Firstly, a small cube box test was done to test the accuracy of the SfM tool. A cube of 12cm*12cm*12cm was taken. In which, random square patterns of different size on each side of the cube was pasted as shown in Figure 4-1.

57 images were taken indoor with proper lighting conditions and enough overlap. The camera setting used was - priority S, ISO 800, shutter speed 1/80 and varying aperture
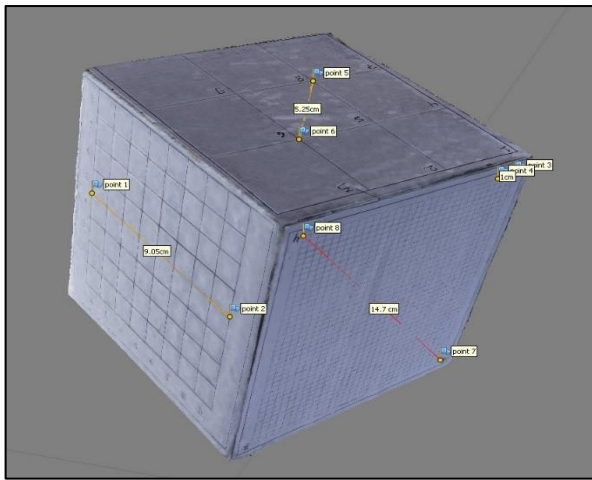
Figure 4-1 Cube Box Sample
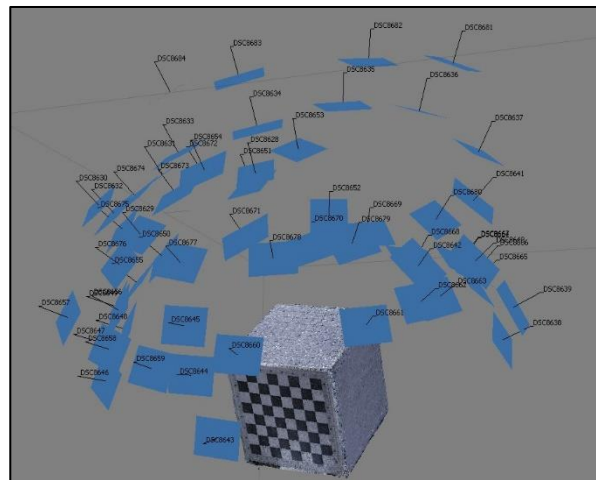
Figure 4-2 Image acquisition in cube box

(f/6.3 to f/14). Figure 4-2 shows the camera position for image acquisition of the cube box.

Agisoft PhotoScan was used for image processing which took 1hr 15min to create a high quality dense cloud with 5.4 million points and 3-D model of 1.06 million faces. The unnecessary noise was deleted to get a fine 3-D model. The 3-D model thus obtained is on a relative scale.

To scale the cube box to an absolute 3-D, few points were marked on the square lining as a reference point on different faces randomly. Point 1 - Point 2 and Point 5 – Point 6 were used for scaling. These points were joined to create a scale bar for scaling. Manually the distance between the points were measured. And the measured distance was given as an input for scaling. Thus, a scaled 3-D cube box is generated. Also, the volume of the cube was calculated manually and compared with the volume output from PhotoScan.

4.1.1 Calculation and Results from cube box test

The length measurement was done in the cube which was compared with the 3-D scaled output. Table 4-1 shows the measured length and estimated length from PhotoScan. RMSE value was calculated following 3.2. The RMSE value is less than 0.5mm. which states that

the scaled output resembles the cube to large extent. Figure 4-3 shows the volume and surface area output from PhotoScan.

Now, for the manual volume calculation, the length of the cube box of all sides were 12 cm, so volume (Vm) = 12cmx12cmx12cm= 1728cm^3

Table 4-1 RMSE of the Cube box test

Points	Manually measured (m)	Photoscan estimation (m)	RSME (mm)	Remarks
Point 1 - Point 2	0.091	0.09100	0	Used for scaling
Point 5 - Point 6	0.053	0.05300	0	Used for scaling
Point 3 - Point 4	0.010	0.01002	0.016	Estimated by photoscan
Point 7 - Point 8	0.147	0.14720	0.2	Estimated by photoscan
Point 9 - Point 10	0.152	0.15150	0.496	Estimated by photoscan
Point 11 - Point 12	0.017	0.01750	0.5	Estimated by photoscan
Point 13 - Point 14	0.159	0.159221	0.221	Estimated by photoscan

In order to calculate the volume from PhotoScan, the fill holes tools must be applied first to fill up the hollow part at the bottom. Since the cube rests on a plain surface so image from the bottom part will be missing which results in a hollow bottom.

Volume output from PhotoScan (Vp)= 0.001720m^3 = 1720 cm^3
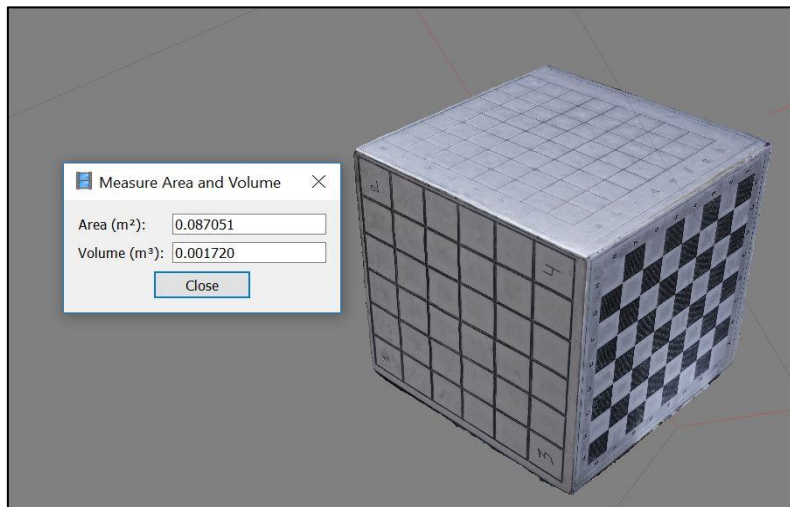
Figure 4-3 surface area and Volume computation from PhotoScan

Difference in volume % $= \frac{Vm-Vp}{Vm} * 100 = \frac{1728-1720}{1728} * 100 = 0.4\%$

Also comparing the total surface area of the cube,

Manual surface area measurement (Am) = 12cm*12cm*6 = 864cm^2

Output from PhotoScan (Ap) = 0.087051m^2 = 870.51cm^2

The difference in total surface area % $= \frac{Ap-Am}{Am} * 100 = \frac{870.51-864}{864} * 100 = 0.7\%$

4.2 Model 1

A physical river model study of the bed evolution at high sediment transport rate was chosen as Model 1. The experiment was carried out in an existing physical model at hydro Lab. A model with a milder bed slope was selected for a better study of bed deformation during high sediment transport event. The model consists of a 20 m long river channel, with a bend, having a longitudinal slope of 1:200. The channel at the upstream end has an average width of 1 m, which then widens to 2 m along the bend and downstream. Only a short reach of this model which consists of a large bent was taken for the study. Detail layout of the model is shown in **Appendix 3**. Channel bed consisted of sediment with a median particle diameter (D50) of 0.55mm and D90 of 1.28mm and geometric standard deviation (σg) of 1.972. The particle size distribution of the sediment is shown in Figure 4-4.
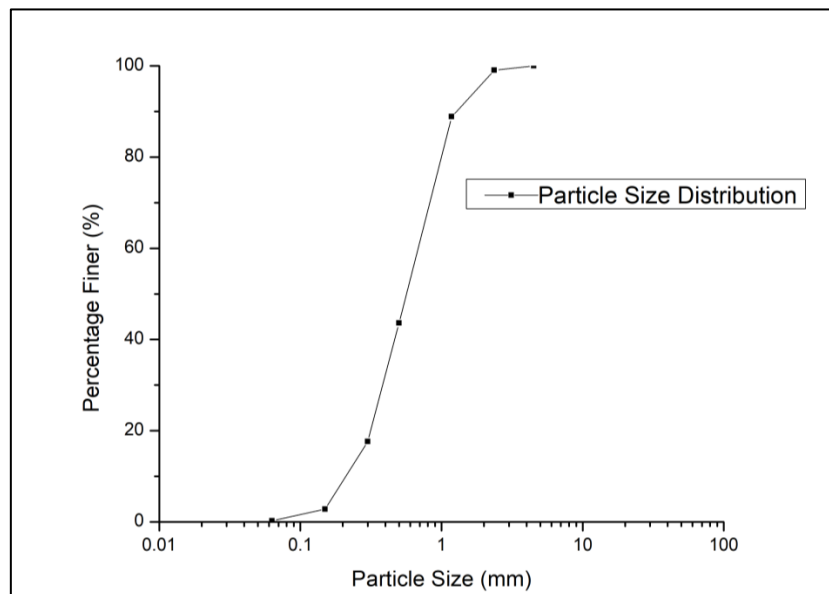
Figure 4-4 Particle size distribution of the sediment used for bed and feed material

4.2.1 Experimental setup

The flow to the model was supplied by pumping water from an underground reservoir to a calibrated V-notch located at the upstream end of the model. Similarly, sediment was fed at the inlet of the model with the help of vibrating type sediment feeder. The water level in the river reach was controlled with the help of a tailgate provided at the outlet. Water falling over the gate was passed through a settling basin - which trapped the sediments exiting the model. The flow exiting the settling basin was then collected into the underground reservoir via a return canal.

The flow was slowly introduced into the model by setting up a high tailgate level which was then lowered to the riverbed level when a steady flow of 40 l/s was maintained in the reach. The sediment feed rate of 10kg/min - estimated using equilibrium bed load transport equation by Meyer-Peter & Müller (1948) for the narrow channel in the reach (see **Appendix 4**) – was then introduced at the inlet. The feed material was the same as that

of the bed material. The experiment was run for 140 minutes until a constant planform was achieved such that it did not vary much over time.

Propagation of sediment deposition from upstream was continuously monitored by a video camera and water levels were recorded at different cross-sections during the experiment. After the experiment ended, the channel bed was left to dry and then manually surveyed to obtain bed level at different cross-sections. Finally, the channel bed was scanned to obtain a continuous surface of the evolved channel bed, using SfM methods discussed on 4.2.2 and 4.2.3.

4.2.2 Data acquisition and georeferencing

Before starting the image acquisition process, 19 GCPs were set in the model which covered the overall area of interest. These GCPs were surveyed manually using a digital theodolite and level machine as discussed in 3.5.1. The accuracy of the surveyed GCPs are shown in Table 4-2. GCP containing higher error (L1) was eliminated to minimize the error. Images were taken with enough overlap of 60% to 70% frontal as well as sideways between the conjugative images. Three different sets of images were taken; the first set for the initial bed of the model, the second set for the initial fill (to speed up the bed formation process) of the sediment and third set of images of the model after running. The number of images taken for each stage is tabulated in Table 4-3. All the images were taken by the same camera with the setting as described in 3.3.

Table 4-2 RMSE in GCPs

GCPs	X (m)	Y (m)	z (m)	Ex(m)	Ey(m)	Ez(m)	$(Ex)^2$	$(Ey)^2$	$(Ez)^2$	RMSE (m)
L1	564033.40	3082229.53	276.28	-0.002	0.0087	-0.002	4E-06	8E-05	4E-06	0.0091
L2	564088.23	3082322.11	285.00	0.0017	-0.003	-0.003	3E-06	1E-05	8E-06	0.0046
L3	564112.71	3082388.69	277.08	-0.003	0.0016	-7E-04	8E-06	2E-06	5E-07	0.0034
L4	564045.27	3082438.90	276.04	-0.002	0.0033	0.0027	4E-06	1E-05	7E-06	0.0048
L5	563948.76	3082496.79	279.96	0.0007	-0.002	-0.003	4E-07	4E-06	8E-06	0.0035
L6	563805.80	3082525.62	278.12	-3E-04	-8E-04	-0.002	7E-08	6E-07	4E-06	0.0022
L7	563687.42	3082494.23	286.28	-3E-04	0.0021	-0.002	1E-07	4E-06	2E-06	0.0026
LA	563954.47	3082173.76	285.56	0.0022	0.0001	-3E-04	5E-06	2E-08	8E-08	0.0022
RA	564139.14	3082131.44	286.68	-4E-05	0.0018	-5E-04	2E-09	3E-06	2E-07	0.0019
R1	564074.59	3082084.29	283.64	0.0018	0.0004	0.0012	3E-06	2E-07	1E-06	0.0022
R2	564177.07	3082193.30	281.16	0.0015	-4E-04	0.0015	2E-06	2E-07	2E-06	0.0022
R3	564259.13	3082322.67	284.36	-0.004	0.0009	-1E-04	2E-05	9E-07	1E-08	0.0045
R4	564299.35	3082449.32	272.12	7E-05	-0.002	0.003	6E-09	3E-06	9E-06	0.0034
R5	564236.49	3082593.01	270.36	0.0005	-0.002	-3E-05	2E-07	4E-06	9E-10	0.0020
R6	564136.98	3082681.72	273.40	-0.001	0.0016	-5E-04	2E-06	3E-06	2E-07	0.0021
R7	564018.43	3082717.86	282.12	-0.001	0.0003	-0.002	2E-06	8E-08	6E-06	0.0029
R8	563853.75	3082725.44	278.04	-9E-04	0.0031	-7E-04	7E-07	1E-05	5E-07	0.0033
R9	563720.05	3082710.24	270.28	0.0008	0.0008	0.0035	6E-07	6E-07	1E-05	0.0037
R10	563601.43	3082682.91	271.48	-4E-05	0.0009	0.0026	2E-09	8E-07	7E-06	0.0028
						SQRT(SUM/N)=	0.0017	0.0018	0.002	0.0030

4.2.3 Processing and Post-Processing

All the three image sets were processed in Agisoft PhotoScan. Firstly, the image sets were loaded into PhotoScan followed by aligning photos and then low dense tie point was created. Then the dense cloud generation process was started. After the dense cloud was generated, unnecessary noise was removed by trimming the dense cloud using selection and delete tool.

A 3-D dense point cloud of relative coordinate was thus obtained. To convert the model into an absolute scale, the coordinates of the reference points (saved as '.txt' or '.csv' format) taken from 4.2.2 were loaded in PhotoScan. Then the GCPs were traced in the images loaded in the model and placed manually to their respective places (see Appendix 2 for detail steps). Thus, after updating the model we got a scaled 3-D final product.

4.2.4 Results and Comparisons

Applying the SfM tool to trace down the sediment transport and bed-form changes, it took less time and effort. The time taken for processing all three sets of images were recorded with the respective size of output point cloud file which is shown in Table 4-3. It took more time to process the initial fill and after running stage since a high-quality dense point cloud was selected. The final output, DEMs of all three different stages are shown in Figure 4-5, Figure 4-6 and Figure 4-7 which shows the deposition of sediments in various stages. Also, the manual length in various random reference points was taken (see **Appendix 7**, figure A) and compared as shown in Table 4-4. The maximum error in length was found to be less than 3mm.

Table 4-3 Processing time and point cloud file size comparison

Stage	GCP	No. of Image	Time for feature matching and alignment	Time to create dense cloud	Quality of dense cloud	Point cloud file size
Initial Bed	19	126	17min	45min	Minium dense	27.17 million
Initial Fill	19	241	40min	12hr 44min	High quality	122.6 million
After run (140min, 40l/sec)	19	116	15min	5hr 8min	High quality	96 million
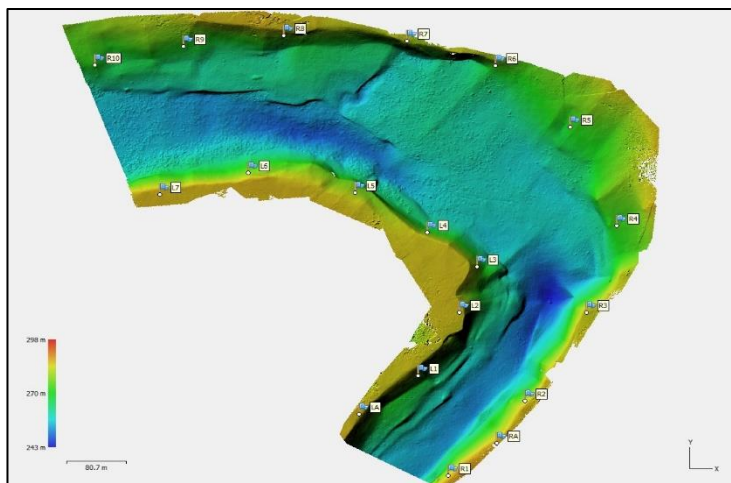
Figure 4-5 DEM of initial bed (model 1)
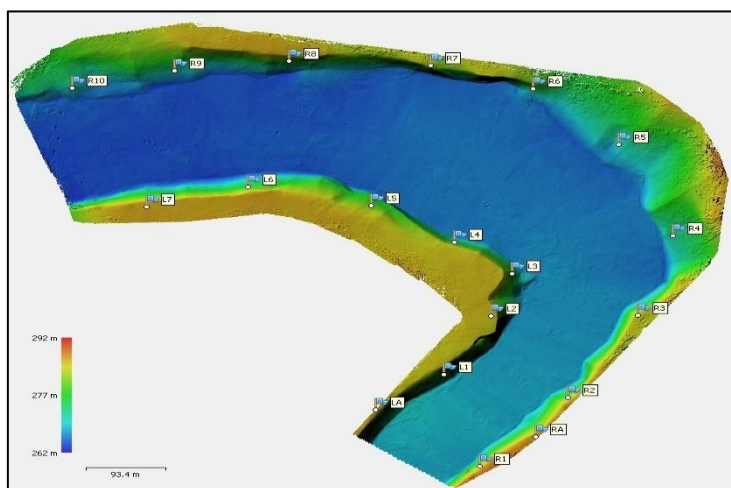
Figure 4-6 DEM of initial fill (model1)
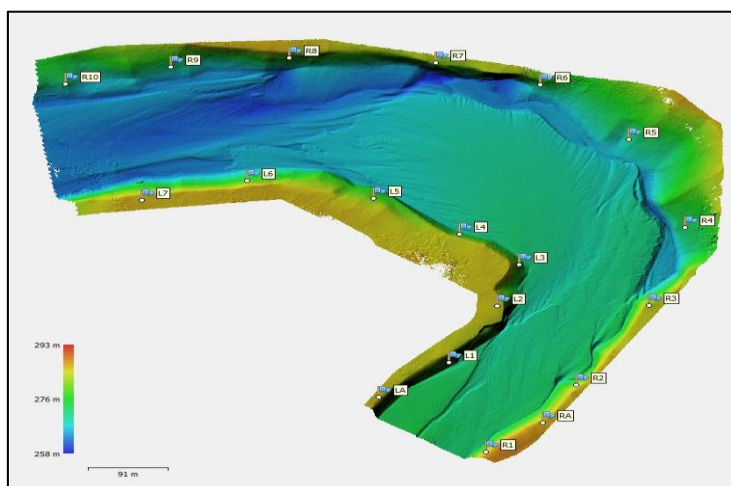
Figure 4-7 DEM after running (model 1)

23

Table 4-4 Measured length comparison with PhotoScan

GCPs	From Photoscan (D) (m)	In Model scale (D/80) (mm)	Manual measurement (Dm) (mm)	Difference |(D-Dm)| (mm)
LA-R1	150.332	1879.2	1877.0	2.15
L1-R2	148.928	1861.6	1862.0	0.40
L2-RA	197.355	2466.9	2465.0	1.94
L2-R3	170.563	2132.0	2135.0	2.96
L5-R5	303.505	3793.8	3796.0	2.19
L5-R9	312.785	3909.8	3912.0	2.19
L7-R10	207.575	2594.7	2597.0	2.31
L6-R9	203.516	2544.0	2544.0	0.05
L5-R7	231.515	2893.9	2895.0	1.06
L6-R8	205.516	2569.0	2571.0	2.05
L4-R6	259.653	3245.7	3245.0	0.66
L5-R4	353.819	4422.7	4425.0	2.27

4.2.4.1 Cross-section comparison

Nine cross-sections were marked in various sections of the model as shown in Figure 4-8and the coordinates of the cross-section points were surveyed (same as coordinates of GCPs). After getting the coordinates of the cross-section, nine cross-sections were cut in the contour map and plotted. The cross-sections were measured manually also as described in 3.5.2. and plotted to compare with the output from PhotoScan. The comparison of the cross-sections is shown in Figure 4-9 and Figure 4-10. The comparison shows that the output from the SfM tool PhotoScan is quite promising to produce more accurate 3-D output.
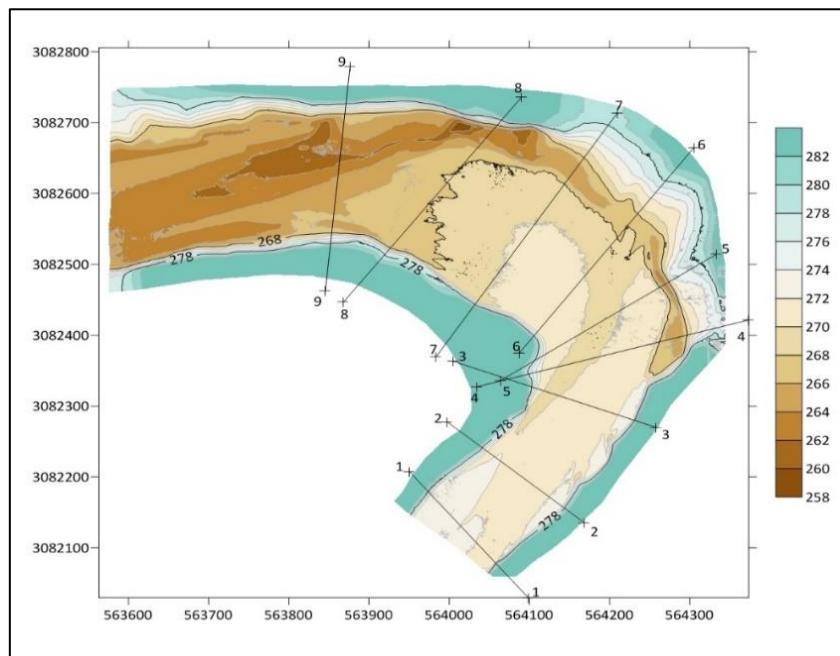
Figure 4-8 Contour map, 2m interval with cross-section plan (Model 1, after run stage)
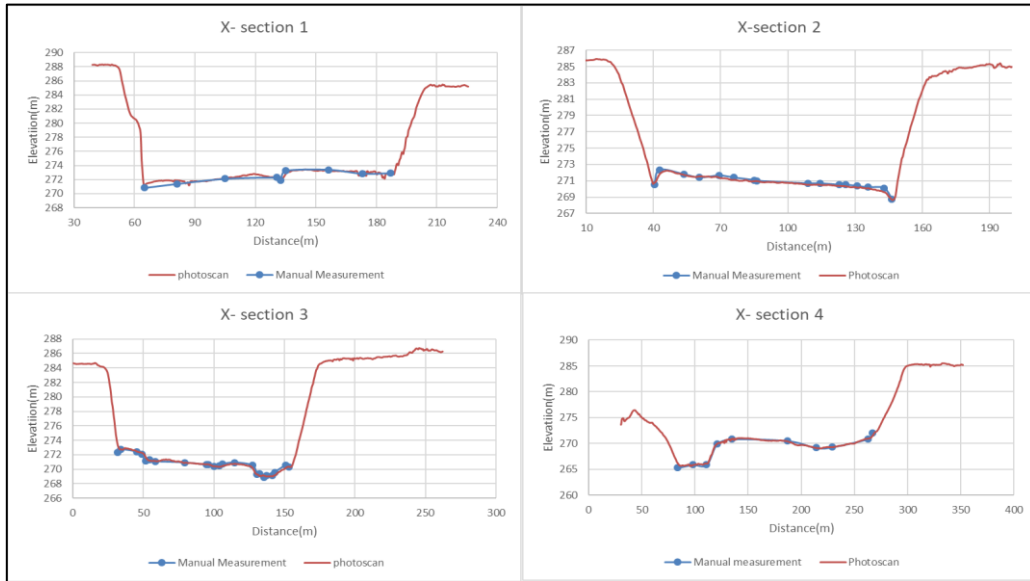
Figure 4-9 Cross-sections (1-4) comparison, Model 1, after run stage
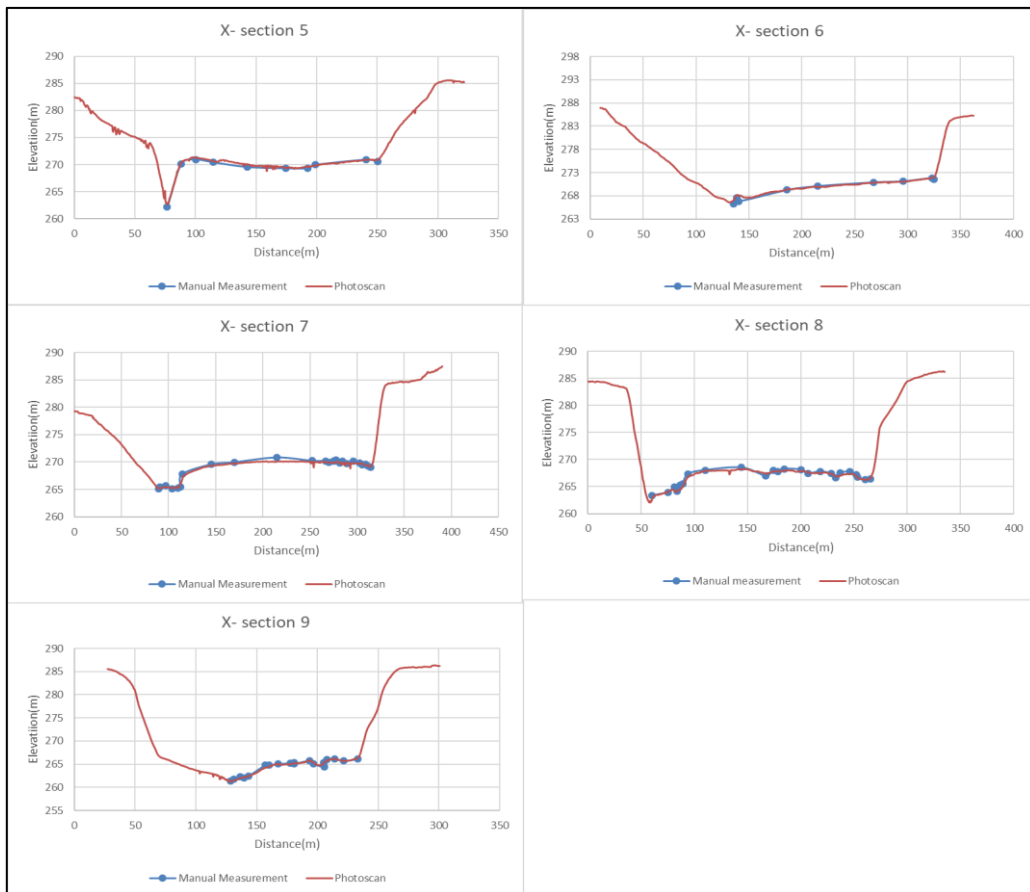
Figure 4-10 Cross-sections (5-9) comparison, Model 1, after running stage

25

4.2.4.2 Volume calculation and comparison

After running the model in 40 l/s flow for 140min, the model was left to dry and the remaining volume of sediment deposit in the bed was measured manually collecting the sediments from inside section 1-1 to section 9-9.

The volume was measured in a round bucket of capacity $0.006m^3$. This volume of sand was filled in a cart of capacity 6 buckets ($6*0.006=0.036m^3$).

The total number of carts filled with sediment was 80.

So, total manual volume measurement=$0.036*80=2.88m^3$

Now, in the same cross-section, the volume of the sand was estimated using cloud compare software. Firstly, the point cloud of the initial bed and final bed in '. ply' format was imported to cloud compare. Both point files were selected and trimmed with the segment tool to match the point file to 99%.

For the volume calculation, 0.4m step and 1733x1574 cell size were selected with 95.2% matching cells.

Thus, the estimated volume (in the prototype scale) from cloud compare was 1,504,462.06 m^3 (Figure 4-11).

Volume in model = $1504462.06/80^3$ = $2.9384m^3$ (model is of 1:80 scale)

Difference in estimation from cloud compare and manual (%) = $\frac{(2.938-2.88)}{2.88} \times 100 = 2\%$
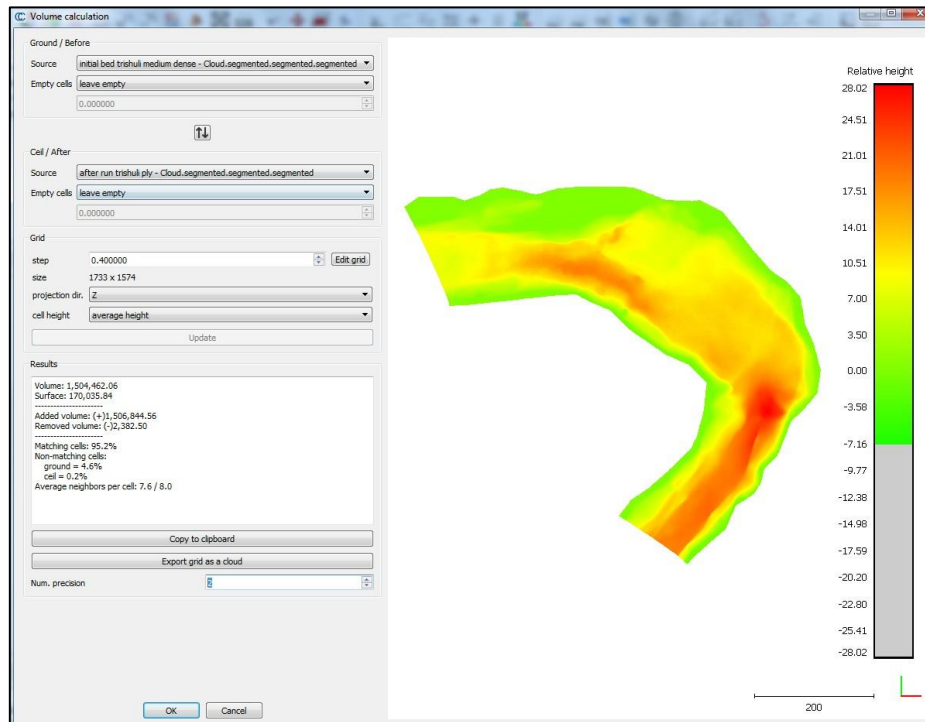
Figure 4-11 Volume estimation using CloudCompare

4.3 Model 2

A physical hydraulic model study of the overall performance test of headworks in a Hydroelectric project (48 MW) was selected as Model 2. The experiment was conducted in an existing model in the Hydro lab. The model was built as an undistorted fixed bed model on a scale of 1:40 using the Froude's Model Law. The headworks design consisted of a free flow type gravity weir, two bed load sluices 5m wide and 6m high, a side intake with eight orifices, a forebay from where water is diverted towards settling basin through two gated inlet orifices- provisioned with a forebay that leads to a flushing tunnel and ultimately discharged at downstream of stilling basin. A general arrangement of the headwork is as shown in Figure 4-12.
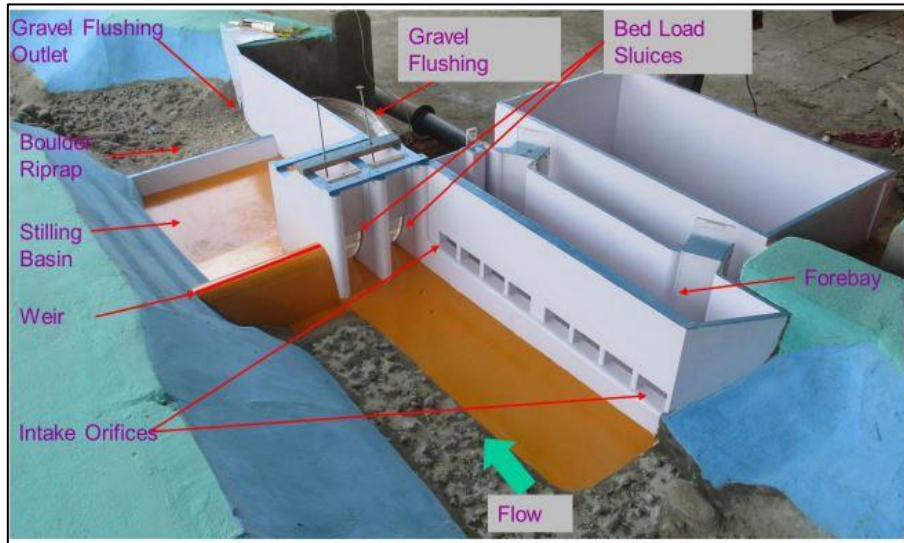
Figure 4-12 General layout of headwork structures, Model 2
(Picture: Hydro Lab)

The main purpose of the test was to know the performance of the structures and calculate the flush volume, mainly during flood scenario with respect to the hydraulics, sediment deposition patterns, and velocities, particularly around the headworks area. The flow selected for this test was an annual flood of 146 m^3/s.

4.3.1 Experimental setup

In order to simulate required discharge in the model, a calibrated discharge measurement box was placed at the inlet tank of the model. Piping arrangements from the pump house to the discharge measuring box were assembled to supply the discharge to the model. The discharge to the power plant, diverted through the intakes, were measured with the help of a calibrated discharge measuring box installed after the settling basins model. Finally, an outlet tank was provisioned at the end of the river model that circulates the flow back to the return canal and then to the reservoir.

Initial fill of sediments was done to speed up the process and a sediment feeder was provisioned at the start of the model to feed measured amount of sediment in the river flow. In order to represent the bedload transport in the river, sediment was fed continuously from the upstream part of the river model during the tests. The adopted rate of sediment fed in the model was 580 g/min.

The floating debris and trashes were represented by small wooden pieces (known sizes) and paper confetti whereas colored dye was used to detect the flow pattern. The particle size distribution of the sediment used is shown in Figure 4-13.

The experiment was run for 12min (8 hours in prototype) for bed formation and 38min (25 hours 20min in prototype) for flushing. SfM tool was applied to scan the different stages of the experiment, i.e. initial bed, initial fill of sediments and final bed after flushing.
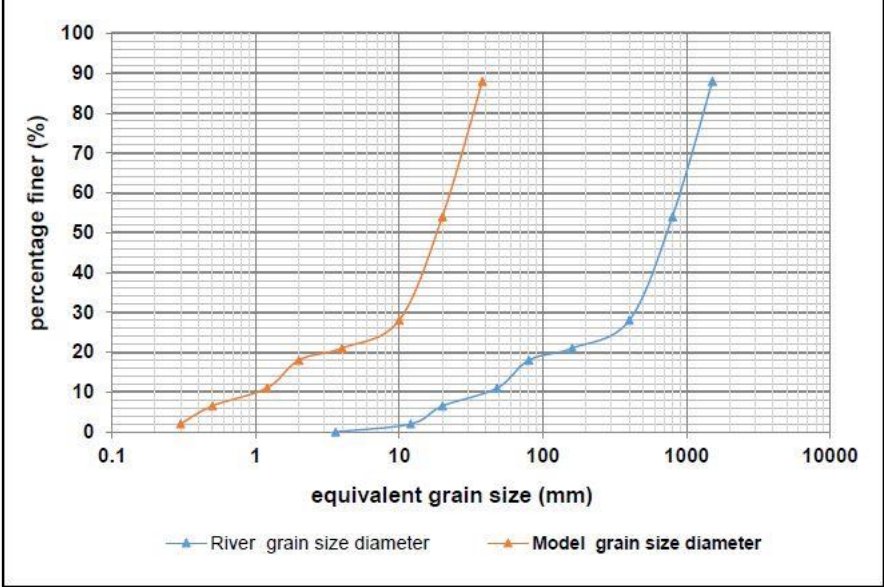
Figure 4-13 Adopted particle size distribution curve PSD (river surface material)

4.3.2 Data acquisition and georeferencing

13 GCPs were set in the model which covered overall area of interest. These GCPs were surveyed manually as discussed in 3.5.1. The accuracy of the surveyed GCP is shown in Table 4-5. GCP R4 and R5 was not used for geo-referencing because of higher RMSE error. Images were taken with enough overlap of 60% to 70% frontal as well as sideways between the conjugative images. The number of images taken for each stage is tabulated in Table 4-6. All the images were taken by the camera and its manual setting described in 3.3.

Table 4-5 RMSE error in GCP (Model 2)

GCP	X (m)	Y (m)	z (m)	Ex(m)	Ey(m)	Ez(m)	(Ex)^2	(Ey)^2	(Ez)^2	RMSE (m)
L1	423674.17	3052047.09	1639.58	-0.00026	-0.00085	-0.00025	6.63E-08	7.2E-07	6.3E-08	0.0009
L2	423714.02	3052047.12	1640.66	0.00020	0.00060	-0.00070	4E-08	3.6E-07	4.9E-07	0.0006
L3	423756.04	3052059.86	1641.22	-0.00053	-0.00075	0.00043	2.76E-07	5.6E-07	1.8E-07	0.0009
L4	423776.06	3052069.62	1645.54	-0.00037	-0.00035	-0.00002	1.33E-07	1.2E-07	4E-10	0.0005
L5	423821.01	3052079.23	1642.38	-0.00011	0.00033	0.00018	1.16E-08	1.1E-07	3.1E-08	0.0003
LA	423693.11	3052058.44	1633.30	-0.00048	-0.00010	0.00120	2.26E-07	1E-08	1.4E-06	0.0005
LB	423794.43	3052087.03	1636.02	0.00024	-0.00014	0.00033	5.64E-08	2E-08	1.1E-07	0.0003
R1	423706.79	3052099.58	1644.12	0.00088	0.00108	-0.00017	7.66E-07	1.2E-06	2.7E-08	0.0014
R2	423740.90	3052100.29	1644.56	0.00004	-0.00043	0.00072	1.37E-09	1.8E-07	5.2E-07	0.0004
R3	423774.54	3052114.42	1645.10	-0.00013	0.00065	-0.00025	1.76E-08	4.2E-07	6.3E-08	0.0007
R4	423807.97	3052140.06	1640.06	-0.02065	-0.00550	0.00813	0.000426	3E-05	6.6E-05	0.0214
R5	423841.15	3052150.81	1642.10	-0.00700	0.00123	0.00128	0.000049	1.5E-06	1.6E-06	0.0071
						SQRT(sum^2/N)=	0.000399	0.00061	0.00054	0.025539

4.3.3 Processing and Post-Processing

PhotoScan was used to process three different sets of images i.e. initial bed, initial fill and after flushing (processing similar as 4.2.3). The time taken for processing all three sets of images were recorded with the output size of the point cloud file which is shown in Table 4-6.

The quality of dense cloud was chosen to low dense in order to speed up the processing speed. A decent amount of point cloud is generated even a low dense quality was selected. Geo-referencing was done using the higher accuracy GCPs (listed in Table 4-5). Further, the point cloud generated was exported in '. ply' file format and imported to CloudCompare for flushed volume calculation.

Table 4-6 Processing time and point cloud file size comparison (Model 2)

Stage	GCP	No. of Images	Time for feature matching and alignment	Time to create dense cloud	Quality of dense cloud	Point cloud file size
Initial Bed	13	106	22min	3hr 58min	Low dense	0.113 Million
Initial Fill	13	61	35min	37min 46sec	Low dense	3.05 Million
After Flushing (38min)	13	74	14 min	47 min	Low dense	3.67 Million

4.3.4 Results and comparison with manual measurements.

SfM was applied to scan the bed and to study the flushing capacity of the structure. The final 3-D output of all the stages are shown in Figure 4-14, Figure 4-15 and Figure 4-16. Also, the manual length in various random reference points were taken (see **Appendix 7**, figure B) and compared as shown in Table 4-7. The maximum error in length was found to be less than 2 mm.
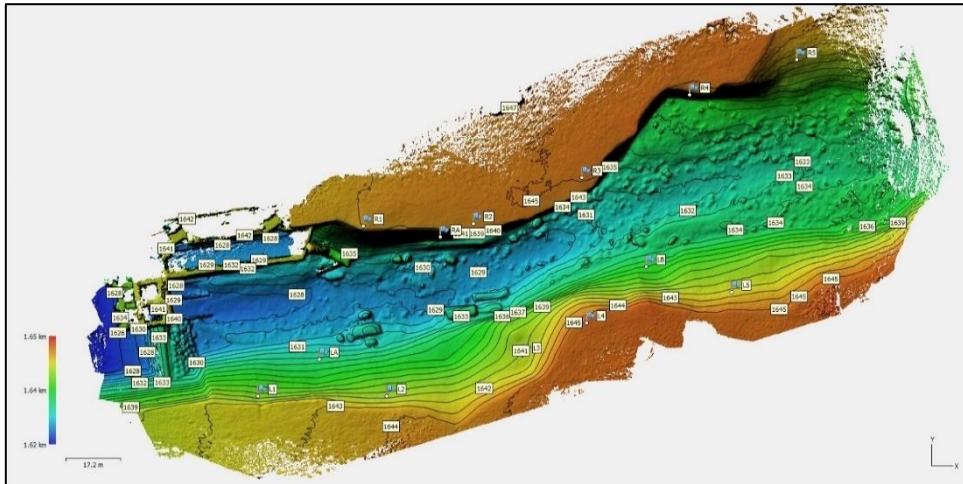
Figure 4-14 DEM of initial bed (model 2)
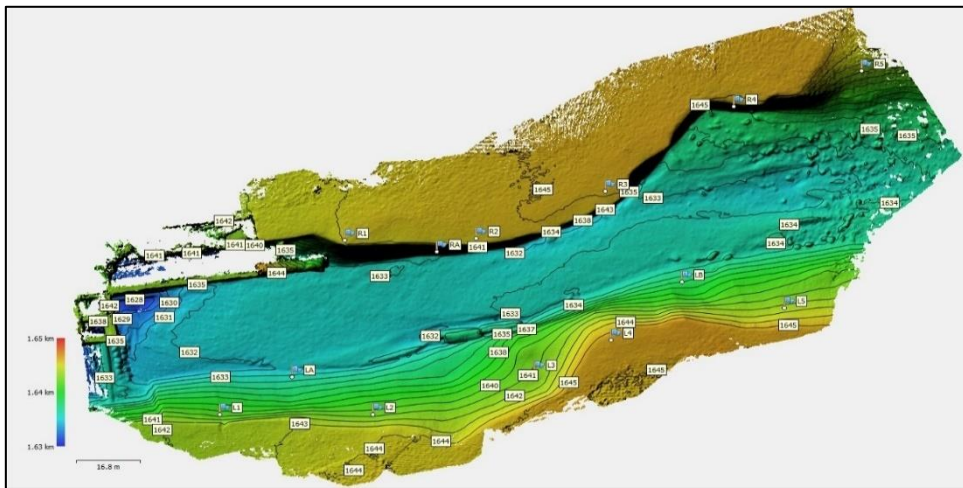
Figure 4-15 DEM of initial fill (model 2)
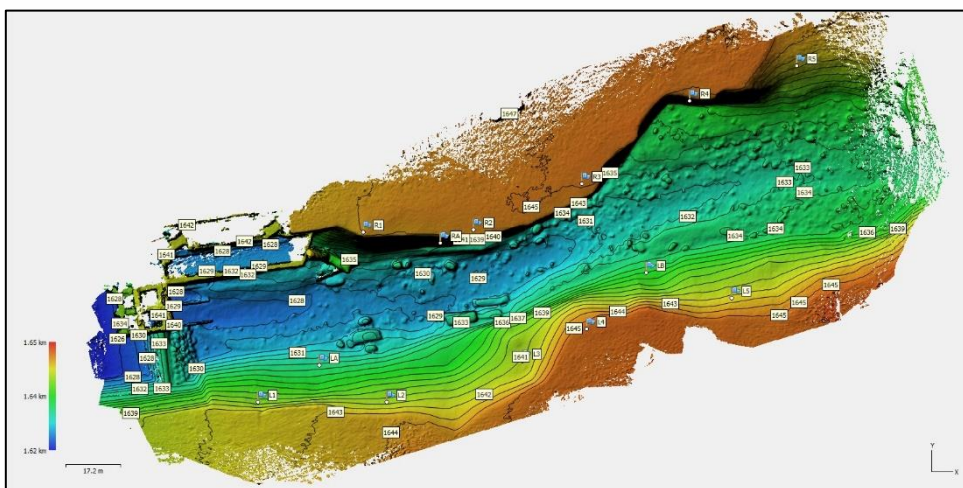
Figure 4-16 DEM of after flushing (Model 2)

30

Table 4-7 Measured length comparison with PhotoScan Output (Model 2)

GCPs	From Photoscan (D) (m)	In Model scale (D/40) (mm)	Manual measurement (Dm) (mm)	Difference |(D-Dm)| (mm)
L1-R1	62.0141	1550.35	1550.00	0.35
L2-R1	53.0727	1326.82	1328.00	1.18
L4-R3	44.8480	1121.20	1121.00	0.20
L5-R5	74.3412	1858.53	1857.00	1.53
L2-R5	164.0584	4101.46	4100.00	1.46
R1-R2	34.0730	851.83	852.00	0.17
R2-R3	36.4788	911.97	913.00	1.03

4.3.4.1 Flush volume calculation and comparison

The flushed volume of sediments was collected in the lower chamber of the outlet of the model. A cube box of 0.3m*0.3m*0.3m (Volume = 0.027 m^3) was taken for measurement. The no. of boxes filled was 6. So, manual volume measurement was 0.162 m^3.

Now, for the volume estimation from cloud compare, all three set of point clouds, initial bed, initial fill and after flush were imported in CloudCompare and trimmed using segment tool (Structure and edges were trimmed, all 3 stages point cloud was trimmed to maintain all cells matching. 99.3% cells were matched). Grid step 0.25 and Grid Size 771*371 was chosen for 2.5D volume calculation, which resulted in the volume 0.1602 m^3.

So, the difference in volume estimation (%) = $= \dfrac{(0.162 - 0.16024)}{0.162} \times 100$ = 1%

5 Results Summary

5.1 Cube box test

Accuracy in the 3-D output can be achieved only if the input parameter for scaling has higher accuracy. Manual length measurement to a millimeter scale might have some error in measurement. Although the cube box test resulted in the RMSE error under 0.5 mm, the volume difference was 0.4% and the surface area difference was 0.7%. This signifies that the resulted 3-D output from the SfM tool (PhotoScan) for a small object is considerably accurate and the 3-D output resembles the physical cube to a large extent. This tool can be used for small object 3-D modeling. Also, it can be a better tool for creating better 3-D models of hydraulic structures in Physical model studies.

5.2 Model 1

Applying the SfM tool in the movable bed scale model (Model 1), it was found that the 3-D model of various stages can be created in less time with much less effort. It took around 12.5 hours to produce a 3-D point cloud of a set of images in the beginning. This was due to the selection of high dense point cloud option. Later, a medium dense point cloud was selected, which took around 45 min to process, producing a fine medium dense point cloud of 27 million points. The RMSE in GCPs was 3mm, which resulted in the maximum length error in the model to be 3mm. The nine cross-sections comparison resulted in a fine overlap between the polylines. Lastly, the volume estimation from PhotoScan variation was only 2% from the manual measurement.

From the model study using SfM tool (comparing the DEMs), it was found that a deposition front of the sediment was observed along the wider reach of the channel, due to reduced sediment transport capacity in wider reach (downstream) compared to the narrow reach (upstream). The deposition front development further extended towards downstream as the experiment progressed. Deposition of sediment was observed along the entire reach with a maximum value of 8 cm in the model and scaling to prototype 8*80=6.4m. The deposition in the channel bed occurred due to higher sediment supply rate than the transport capacity of the channel. The deposition of sediment was not uniform along the cross-section because of the bend. High sediment deposition was observed along the left bank (inner bend) than the right bank (outer bend). This is attributed due to secondary flows in bend. The accuracy of cross-sectional data by SfM has profound importance in river morphological studies. Study related to the formation of dunes, anti-dunes or bars can be done with such data. In addition, the data obtained by SfM can be used for numerical simulation of the river reach. For example, bathymetry data can be obtained from the point cloud for numerical simulation in Delft3D.

5.3 Model 2

Unlike Model 1, Model 2 consisted of complex hydraulic structures. Applying SfM in Model 2, the overall performance of the headwork was tested. All the three stages of the model bed were scanned using SfM tool and the output was compared. The maximum variation in length measurement was found be less than 2 mm from the manual measurement. The flushed volume calculated by the SfM tool was 0.1602 m^3, which varied just 1% from the manual measurement of volume i.e. 0.162 m^3.

From the experiment, it was found that floating debris was observed to be rotating in front of bed load sluices and trash racks. With sediment deposit in front of the intake orifices, a significant amount of sediment was entered and deposited in the forebay. The forebay flushing gate was capable of clearing deposits only close to its vicinity but rest of the deposits could not be flushed. A submerged jump occurred in the stilling basin with a skewed jump along the left bank. The intensity of jump at the downstream of end sill increased which could cause erosion of the boulder riprap. In addition, the flow depth near the outlet of forebay flushing tunnel was about 1.5 m high, due to the submergence effect. The design discharge with an additional 20 % for flushing discharge was maintained by opening 2 m and 1 m left and right bed load sluices respectively and closing the forebay flushing gate. Only one and half of another intake orifices at the downstream side could be kept open during the operation. The bed load sluices were incapable of controlling bed load deposited in front of the intake that eventually resulted in clogging of the intake orifices over time. With the clogging of the intake orifices with sediments over time, abstracting design discharge for power generation and sediment flushing was not possible during the annual flood of 146 m^3/s. Comparing the DEM output of the initial stage and final stage we were able to trace the amount and location of unflushed sediments.

The accuracy in the calculation of sediment flushing volume has special significance in the development of sediment transport models. Currently developed sediment transport models only predict sediment transport at sub-critical flows. Prediction of sediment transport at super-critical flows is a challenging task. The high-resolution DEM obtained using SfM technique can be used to validate sediment transport models for predicting flushing volume of sediments by bedload sluices and sediment transport during floods.

6 Discussion and Conclusion

Image acquisition was a key factor for a better quality 3-D model generation. Sharper and detailed images produced a fine quality 3-D model. For this, a better and uniform lighting condition in the model was needed to be maintained. A model containing water patches needs to be avoided either by draining or drying the surface. The water patches resulted in a reflection in the images and finally, the 3-D output consisted of a void area.

The model with hydraulic structures consisted of a non-textured shiny and unicolor paint. Glass surface was also used for some of the structural parts of the hydraulic model. Due to this unicolor and non-textured surface, the resulted 3-D output consisted of a hollow space in the structure area. To avoid this a better angle for image capturing was selected followed by a series of close shots of the structures.

Another factor was the error in the measurement of GCP. It played a vital role in the accuracy of the model. Higher the error in GCP, the scaled model was more inaccurate. Two angle measurement was chosen to avoid the error in X and Y coordinate in GCP, followed by the elimination of the GCP having higher RMSE. The results from model 1 of scale 1:80 and model 2 of scale 1:40 showed that the RMSE error increased with the increase in model scale ratio.

The volume estimation in both model cases compared to the manual measurement had a higher accuracy. The volume was estimated subtracting the DEM of initial bed from the final bed, so due to the relative error in both initial and final bed resulted in better accuracy in volume estimation.

This study points the value of using novel techniques for the generation of digital elevation models, particularly the SfM technique approach was employed here. SfM tool 'Agisoft PhotoScan' is highly advanced software which generates very accurate dense cloud, the other features such as cleaning the dense cloud or building a mesh are also handy.

This research furthers our conceptual understanding of sediment transport in physical hydraulic models in various stages and flow conditions. The study concludes that the SfM tool can be applied to the movable bed scale models. It is a very reliable and efficient tool to capture 3D geometry of a physical hydraulic model providing a better result in a shorter period with less effort. The cross-sections and profile of the model bed can be generated in no time with reliable accuracy. The error in the output was in a few millimeters, this states that the model designed to accept this error range in the model can implement this method. The volume estimated by SfM was quite promising. So, for the calculation of flushed volume and estimating existing volume, this tool can be beneficial.

7 Porposal for future work

The tests for this study was done in the model scale 1:40 and 1:80 only. More studies with a wider scale ratio can be done to confirm the obtained results as well as to see the effect of scale in the accuracy of the output obtained.

Only six software were compared and among them, a commercial software 'Agisoft PhotoScan' was chosen for the study. For further studies, other SfM tools besides this can be compared.

Also, the output from the SfM tool comparison with a laser scanner, acoustic transducer systems, and manual measurement parallelly would give a clear picture of the accuracy of the expensive tool and an affordable tool.

The study of SfM in a model containing partially or full water is likely to be useful in future studies. Application of SfM in the hydraulic flume studies would be an interesting study for the future.

References

Agisoft. (2019). Retrieved from Agisoft: https://www.agisoft.com

Agisoft PhotoScan User Manual: Professional Edition, Version 1.4. (2018). Copyright © 2018 Agisoft LLC.

Alfredsen, K. (2018). Brief Communication: Mapping river ice using drones and structure from motion. *The Cryosphere*.

Arya, S. (1998). An Optimal Algorithm for Approximate Nearest Neighbor Searching in Fixed Dimensions. *Journal of the ACM*.

Autodesk, Photogrammetry Software. (2019). Retrieved from Autodesk: https://www.autodesk.com/solutions/photogrammetry-software

CloudCompare. (2019). Retrieved from cloudcompare.org

Dessler, W. (2018, October). Retrieved from GIS Resources: http://www.gisresources.com/common-business-uses-photogrammetry/

Fischler, M. A., & Bolles, R. C. (1981). Random Sample Consensus: A Paradigm for Model Fitting with Applications to Image Analysis and Auomated Cartography. *Communications of the ACM*.

Furukawa, Y. (2010). Towards Internet-scale Multi-view Stereo. *Computer Society Conference on Computer Vision and Pattern Recognition*.

Furukawa, Y., & Ponce, J. (2007). Accurate, Dense, and Robust Multi-View Stereopsis. *CVPR, IEEE Computer Society Conference on Computer Vision and Pattern Recognition. IEEE Computer Society Conference on Computer Vision and Pattern* (p. 8). ResearchGate.

Goldstein, E. B. (2015). Ground control point requirements for structure-from-motion derived topography in lowslope coastal environments.

Horn, B. K. (1987). Closed-form solution of absolute orientation using unit quaternions. *Journal of the Optical Society of America A*.

James, M., & Roboson, S. (2012). Straightforward reconstruction of 3D surfaces and topography with a camera: Accuracy and geoscience application. *Journal of Geophysical Research: Earth Surface*.

Lohani, B., & Mason, C. D. (2001). Application of airborne scanning laser altimetry to the study of tidal channel geomorphology. *Journal of Photogrammetry and Remote Sensing*.

Lowe, D. G. (2004). Distinctive Image Features from Scale-Invariant Keypoints. *International Journal of Computer Vision*.

Micheletti, C. N., & Lane, S. N. (2015). Investigating the geomorphological potential of freely available and accessible structure-from-motion photogrammetry using a smartphone.

Micheletti, N. (2015). Structure from Motion (SfM) Photogrammetry. *British Society for Geomorphology*.

Milan, D. J. (2007). Application of a 3D laser scanner in the assessment of erosion and deposition volumes and channel change in a proglacial river. *EarthbSurface Processes and Landforms*.

Nocedal, J., & Wrighr, S. J. (1999). *Numerical Optimization.* New York: Springer.

Nyimbili, P. H. (2016). Structure from Motion (SfM) - Approaches and Applications. *INTERNATIONAL SCIENTIFIC CONFERENCE ON APPLIED SCIENCES*.

Oniga, V.-E. (2018). Determining the Optimum Number of Ground Control Points for Obtaining High Precision Results Based on UAS Images †. *Proceedings*.

PIX4D support. (2019). Retrieved from PIX4D support: https://support.pix4d.com/hc/en-us/articles/202557459-Step-1-Before-Starting-a-Project-1-Designing-the-Image-Acquisition-Plan-a-Selecting-the-Image-Acquisition-Plan-Type#label1

Sanvely, N., Seitz, S. M., & Szeliski, R. (2006). Photo Tourism: Exploring Photo Collections in 3D. *ACM Transactions on Graphics*.

Shapiro, L. G., & Stockman, G. (2001). *Computer Vision, pp Prentice-Hall.* New Jersey, USA.

Shervais, K. (2016). Structure from Motion (SfM) Photogrammetry Field Methods Manual.

Snavely, K. N. (2008). *Scene Reconstruction and Visualization from Internet Photo Collections.*

Szeliski, R., & Kang, S. B. (1994). Recovering 3D Shape and Motion from Image Streams using Non-Linear Least Squares.

Theia-sfm.org. (2016). *Structure from Motion (SfM)*. Retrieved from Theia Vision Library.

Westoby, M. (2012). Structure-from-Motion, photogrammetry: A low-cost, effective tool for. *Geomorphology*.

Yang, M.-D. (2012). Image-based 3D scene reconstruction and exploration in augmented reality. *Automation in Construction*.

Appendices

Appendix 1: A conference paper written in "Application of 'Structure from Motion' (SfM) technique in physical hydraulic modelling".

Appendix 2: Image processing and Scaling steps in PhotoScan.

Appendix 3: Detail layout of the physical model of a reach of the river.

Appendix 4: Sample calculation for discharge and sediment transport feed

Appendix 5: Sample calculation of GCP (X, Y) manually

Appendix 6: Sample calculation of GCP (Z) manually

Appendix 7: Random manual distance measurement in model 1 and model 2

Application of 'Structure from Motion' (SfM) technique in physical hydraulic modelling

Sanat Kumar Karmacharya[1,2], Meg Bishwakarma[2], Ujjwal Shrestha[1] and Nils Rüther [*1]

[1]*Department of Civil and Environmental Engineering, NTNU, Trondheim, Norway*

[2]*Hydro Lab Private Limited, Lalitpur, Nepal*

* Corresponding author (nils.ruther@ntnu.no)

Abstract. There are many methods available for measurement of bed morphology in physical hydraulic model studies considering mobile bed sediment. Among which, there are sophisticated instrumentations which provide quality results in shorter time but are vastly expensive and requires special training for execution. Whereas the conventional surveying methodology, which is simple and inexpensive, requires plenty of time for the measurement and processing of the data. That is why the recent developments in 'Structure from Motion' (SfM) technique have made it a potential candidate for an inexpensive and efficient tool for measurement of bed morphology in physical hydraulic model studies. SfM method allows to simultaneously determine both the parameters of the camera and the 3D structure of a scene by combining 2D images taken from multiple viewpoints. SfM tools can create a dense point cloud out of a set of partially overlapping photographs taken even by a budget friendly digital camera. The SfM method have already been used as an alternative for topographic surveying to create high-resolution digital elevation models (DEM). Some researchers had also used it for measurement of bed morphology in laboratory experiments. In this study, different freely available SfM tools were used to create a dense point cloud from a set of photographs representing a short reach in a river model in the hydraulic laboratory at Hydro Lab. The selected tools were compared with each other and against a commercial software, based on the methodologies used, processing time and quality of the output. Then the results from SfM method were compared with actual measurements in the physical model done with a conventional surveying technique using a theodolite and a level machine. The results showed that free SfM tools can also produce efficient results compared to commercial tools and SfM method can be used as an inexpensive and efficient alternative for bed morphology measurements in physical hydraulic models.

1. *Introduction*

With aggressive advancement in technology, currently various methodologies are available, over conventional ground surveying techniques, for creating a high-resolution digital elevation models (DEM) of a topography. Aerial photogrammetry, airborne lidar and ground based terrestrial laser scanners (TLS) are some advanced technologies, which have revolutionized the quality of DEMs extending their spatial extent, resolution and accuracy [1]. Recently, easy access to unmanned aerial vehicles (UAV) and drones has made the aerial imaging surveys more convenient and inexpensive.

Besides the development in large-scale terrestrial surveying, there has also been a huge advancement in data acquisition and processing technologies for hydraulic laboratories. Producing DEMs of physical

hydraulic models and/or recording bed morphologies in fluvial sediment transport studies in hydraulic laboratories can be carried out more accurately by using laser scanning or acoustic sounding systems. These systems can be tailored for semi or fully automatic data acquisition curtailing the experiment time. Despite these sophisticated instrumentations are useful in producing high quality DEMs in shorter time, they require high logistical cost and specialized user expertise. Therefore, many hydraulic laboratories still use conventional measurement techniques that are inexpensive and simple though more time demanding. In conventional techniques, measurements are taken at selected points/cross-sections and those data are interpolated in-between. The accuracy of such measurements can be improved by increasing the density of measured points especially at desired details to be captured but it will ultimately increase the time required for measurement and data processing. On the contrary, the laser and acoustic scanning can record highly dense point cloud in shorter time ensuring higher resolution DEM.

In this study, an advanced yet inexpensive and easy to perform photogrammetric method, called 'Structure from Motion' (SfM), was used to produce high resolution DEM of a physical hydraulic river model. Basic principle governing SfM method is similar to stereoscopic photogrammetry in which a 3D structure is developed from a series of overlapping 2D images [1]. Unlike conventional photogrammetry, SfM method utilizes advanced algorithms by which it automatically solves the relative camera positions, orientation and geometry of the target object based on the features extracted from the set of images [2]. Possibility of using low-cost consumer level digital cameras and availability of free and open-source processing tools has given SfM method boundless potentials. Nowadays, SfM has already been widely used in various fields like archaeology, geosciences, robotics, terrestrial surveying, real state, film and entertainment, sports etc. The possibility of using SfM method in an inexpensive and simple way to record 3D information from laboratory models was assessed in this study.

2. *Methodology*

2.1. Structure from motion (SfM)
There are various algorithms available for application of SfM but the general principle remains the same and has been described by [1] [3] and [4]. SfM requires a set of overlapping images, capturing the object from multiple viewpoints, as an input. From the images, common feature points across the image set called key point descriptors are identified using a scale invariant feature transform (SIFT) algorithm. With these feature points and camera parameters extracted from the images, camera location, orientation and position of the feature points are simultaneously resolved in a relative 3D coordinate system. Once the spatial positions of the images are established, a sparse bundle adjustment (BA) algorithm is used to create 3D points covering the area of interest. Then, dense point cloud is produced by intensifying the sparse point cloud with multi view stereo (MVS) techniques. Once the dense point cloud is obtained, it can be used for further processing like developing a DEM, mesh generation, creating a 3D model etc. as per requirement.

2.2. Software
Nowadays, due to the application of SfM method in diverse fields, there are various software available for its implementation. Following six software were selected for application of SfM method in this study. First two are commercial software whereas remaining four are free to use.

2.2.1. PhotoScan.
PhotoScan (now available as Metashape) is commercial software developed by Agisoft LLC, Russia. It is an easy to use stand-alone software which offers all the capabilities from processing images to 3D model generation and texturing and includes additional pre-processing and post processing features. Professional edition of the software is priced USD 3,499 and the standard edition is available for USD 179. However, standard edition itself is enough for generation of 3D models and lacks only other extra features that professional edition offers.

2.2.2. ReCap.
ReCap (named after abbreviation of Reality Capture) is developed by Autodesk Inc USA and is a cloud-based service tailored for generation of 3D models from photographs or laser scans. ReCap Photo, which is included within ReCap pro, is specifically targeted for support UAV and drone photo capture workflows. ReCap Photo can be used to create photo textured meshes, photo-based point clouds with geo-location and high-resolution orthographic views with elevation maps. It can also be

used in object mode to create 3D models of objects. It is a commercial software and ReCap pro subscription is needed to use the service. The subscription costs USD 40 for a month, USD 305 for a year and USD 915 for three years. The service uses cloud credits for each projects and additional cloud credits can be purchased separately once subscribed. Currently, ReCap pro subscription allows you to process up to 1,000 images for one project in aerial mode while the limit is 300 photos for one project in object mode. The software can be used freely under academic license but has the limitation of 100 photos for one project and academic users may also have to wait in long queue for processing. Since it is a cloud-based service, no expensive hardware is required for the processing and the images can be uploaded via smartphone app too. The disadvantage could be it works like a black box and users have very limited control over the quality of the output.

2.2.3. VisualSfM. VisualSfM, developed by Dr. Changchang Wu, is a GUI application for 3D reconstruction using structure from motion (SFM). The reconstruction system integrates different algorithms like SIFT on GPU (SiftGPU), Multicore Bundle Adjustment and Towards Linear-time Incremental Structure from Motion [5–7]. VisualSFM runs fast by exploiting multicore parallelism for feature detection, feature matching, and bundle adjustment. It is one of the first free photogrammetry program to utilize the power of graphical processing unit (GPU). It can process up to sparse reconstruction and utilizes Yasutaka Furukawa's PMVS/CMVS tool for dense reconstruction, which has to be integrated and can be run from the VisualSfM's GUI. However, the sparse point cloud from VisualSfM can be processed in other dense reconstruction tools as well to produce dense point cloud. VisualSfM is free and open source but the licensing restricts its commercial use.

2.2.4. Regard3d. Regard3d is a free and open-sourced structure from motion software which is developed by Roman Hiestand. It offers complete SfM processing up to dense point cloud generation. It can also generate surface, from the dense point cloud, either with colored vertices or with a texture. It has integrated several algorithms and users have a bunch of options to control the quality of the output.

2.2.5. Meshroom. Meshroom is a free and open-source 3D reconstruction software based on the Alice Vision framework. It can perform complete 3D reconstruction up to textured surface creation. It has a node-based workflow that gives its users a lot of control on setting the processing and once its set whole processing can be completed in one click. The advantages of this software are it supports augmented reconstruction i.e. more pictures can be added for better detailing while the processing is on-going. Additionally, it can also perform live reconstruction. The disadvantage of Meshroom could be that it requires CUDA enabled GPU with at least computing capability of 2.0. It should be noted that it does not warn users if they lack the mandatory GPU requirement and the processing seems to be frozen without any notifications. Despite of its promising features and capabilities, there is not any official user manual or guide available yet.

2.2.6. COLMAP. COLMAP is a free and open-sourced Structure-from-Motion (SfM) and Multi-View Stereo (MVS) pipeline with a graphical and command-line interface. It offers a wide range of features for reconstruction of ordered and unordered image collections [8]. It uses MVS technique for dense point cloud reconstruction and uses screened Poisson surface reconstruction algorithm to recover 3D surface geometry from the dense point cloud. However, COLMAP requires CUDA-enabled GPU (at least CUDA version 7.x) to perform dense reconstruction and surface creation processes. But processes up to sparse reconstruction can be carried out without CUDA-enabled GPU and the output can be exported to do dense reconstruction with other tools. For beginners, COLMAP has an automatic reconstruction tool that simply takes a folder of input images and produces a sparse and dense reconstruction in a workspace folder.

2.2.7. Meshlab. Meshlab is the open source software for processing and editing 3D point clouds and 3D triangular meshes and creating 3D models [9]. In this study, Meshlab was used for transformation of 3D dense point cloud in arbitrary coordinates created by SfM software to 3D dense point cloud in actual coordinates.

2.3. Hardware

2.3.1. Camera. Sony α6300 (model ILCE-6300) camera was used for taking pictures for this study. It was a mirrorless digital camera with 24-megapixel Exmor RS sensor, and 425 phase detection autofocus points. The camera setting has a significant impact on the image quality which ultimately affects the quality of the output. After various trials with different settings, following camera settings were used for this study:

- Shooting mode: Shutter Priority (S)
- Shutter speed: 1/80 sec
- ISO: 640
- Aperture: F9-F11
- Focal length: 16 mm
- Image format: JPEG

2.3.2. Workstation. The specification of the workstation determines the total processing time except for the cloud-based processing as with ReCap. For fair comparison, same workstation with following specifications were used for processing with all the selected software:

- Operating System: Microsoft Windows 7 Ultimate 64-bit
- Processor: Intel® Core™ i7-4790 CPU @3.60GHz
- Installed memory (RAM):   32 GB
- GPU: NVIDIA GeForce GTX 750 Ti -18 GB available memory

2.4. Ground control points (GCPs)

With SIFT algorithm, the 3D structure is created based on relative spatial relationships between the original image locations in an arbitrary 3D coordinate system [10]. That means the structure (shape) of the object is recovered but the size is scaled to some arbitrary scale factor. Hence, the final output, either the dense point cloud or 3D surface model, must be transformed using rotation, translation and scaling. To perform this transformation, several ground control points (pre-defined set of points with known coordinates) are needed in the study area. For large scale terrestrial surveying, in order to obtain high accuracy of final output (RMSE<1) 1GCP per 200m^2 is needed to be placed in the interest area [11]. But, at least 5 control points are needed to acquire a precise 3D point cloud [12]. Total 8 control points were used in this study and these control points were marked such that it covered all the concerned area. Image acquisition process was started after setting the control points. Also, it is possible to get a scaled final product without placing manual markers if the images from a GPS enabled camera is used for processing. However, the manual marker placement with pre-defined coordinate system is usually more accurate allowing more precise geo-referencing.

3. Case Study

3.1. Study area

A small reach of a physical hydraulic model of a river, in the hydraulic laboratory of Hydro lab at Kathmandu, was taken as the object for this study. The model was built in 1:40 scale. The length of the study area is about 3 m which represents 120 m long river reach in prototype. Eight ground control points covering all the region was marked on the model as shown in the Figure 1.
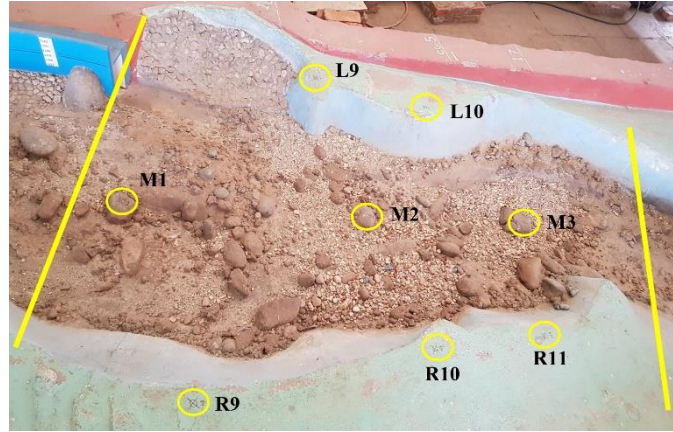
Figure 1. A small reach of a river model in Hydro Lab used as object for this study

3.2. Image acquisition

Several images were taken from varying camera position and angle covering the whole study area. Few close-up images of the boulders were also taken to obtain better detailing. It was ensured that there was enough light in the model with no direct sunlight and sharp shadows. Each feature and control points were captured in at least three images from different viewpoints.

3.3. Image processing and dense reconstruction

At first, the images were filtered removing very bright, dark, blurred and shadowed images if any. 46 images were selected for further processing. The set of images were processed using all the selected software individually and 3D dense point clouds were created. Meshroom and ReCap created 3D mesh as output, which were later converted to 3D dense point cloud using Meshlab. Total time for feature extraction/feature matching, sparse reconstruction and dense reconstruction by each software was recorded and compared as one of the major performance parameters. The processing time up to dense reconstruction for the selected software is shown in Table 1. The processing was done mostly with default settings of the software to assess the possibility of using them by a complete beginner.

Table 1. Processing time up to dense reconstruction for selected software.

Tools	Feature extraction and Feature matching	Sparse reconstruction	Dense reconstruction	*Total processing time*
Colmap	1 hr 51 min	31 min	8 hr 4 min	10 hr 26 min
Meshroom	2 min	3 min	1 hr 41 min	1 hr 46 min
PhotoScan	5 min		3 hr 34 min	3 hr 39 min
ReCap	-	-	-	2 hrs
Regard3d	1 hr 38 min	29 min	35 min	2 hr 42 min
VisualSfM	3 min	31 sec	24 min	58 min

3.4. Post processing

The 3D dense point clouds created by the selected software were transformed from arbitrary 3D coordinates to the real prototype coordinates (not model coordinates) using rotation, translation and scaling in reference to the coordinates of GCPs. It was done in Meshlab using 'roto-translation' with 'uniform scaling' in geo-referencing tool. During the transformation, GCPs with error (RMSE) greater than 1 were eliminated to ensure better accuracy [13]. Thus, the georeferenced point cloud is generated. The point cloud data was exported to create a contour map with 1m X 1m grid resolution as shown in Figure 2.

3.5. Manual measurements

For assessing the accuracy of outputs by selected software, 4 cross-sections in the river model were manually measured using a level machine and bar scale. These cross sections were compared with the corresponding cross-section profiles extracted from the contour plots produced by using dense point clouds from the selected software.
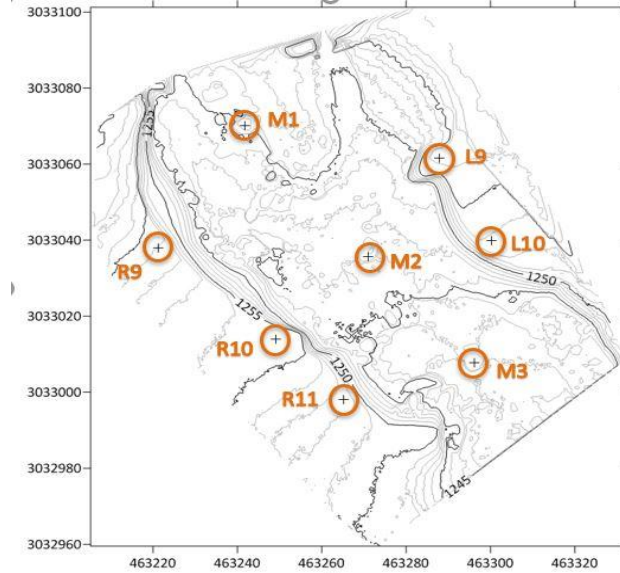

Figure 2. Contour Map plotted from 3D point cloud created by PhotoScan

4. *Results and discussion*

It was observed that SfM method created high density point cloud thus captured better details compared to the manual measurement. The total number of points in the final 3D dense point clouds vastly varies from 2.03 million for Meshroom to 29.2 million for PhotoScan. Although point cloud by Meshroom contained minimum number of vertices, the quality of the output was not lesser. Hence, bigger number of vertices may not necessarily mean better quality of the output. The final output by each software and the total number of vertices forming the 3D output are shown in Figure 3. Finally, 4 cross-sections profiles within the study area were extracted from the contour map plotted using 3D dense point cloud from each software. Each of the cross-section profiles were plotted together with that obtained from manual measurements and compared with each other as shown in Figure 4 where comparison for two cross-section profiles are shown. The plots show that the cross-section profiles generated with selected SfM tools are in close agreement with each other and with the manually measured cross section profile.

To quantify the capability of the SfM tools to predict the vertical dimension, elevation of the 150 points, where manual measurements were done, were extracted from the point clouds generated by each of the selected software. Those elevations were compared with measured elevations and mean absolute error (MAE), root mean square error (RMSE) and coefficient of determination (R^2) were calculated as shown in Table 2. It is to be noted that MAE and RMSE values shown in Table 2 are in meters as the analysed results were in prototype scale. The results show that each of the selected software is good at predicting the vertical dimension with MAE below 0.24 m and RMSE below 0.30 m in prototype scale which represents MAE below 6 mm and RMSE below 7.5 mm in model scale. Here, PhotoScan stood out as 'the best among equals' by scoring lowest MAE and RMSE, and highest R^2 value. However, the quality of results are dependent on various factors like choice of different algorithms and respective parameter values within SfM technique,

resolution of DEM generated from dense point cloud and accuracy of GCPs used for geo-referencing. Also, the acceptable limit for error or discrepancies varies with the purpose of the model study, scale factor and measurement techniques. Therefore, there is an immense possibility to obtain better results with free and open source software by tweaking various parameters whereas commercial software like PhotoScan and ReCap work as a black box model and give their users lesser control. On the other hand, PhotoScan and ReCap are user friendly, easy to use and can deliver quality results with minimum involvement of the user.
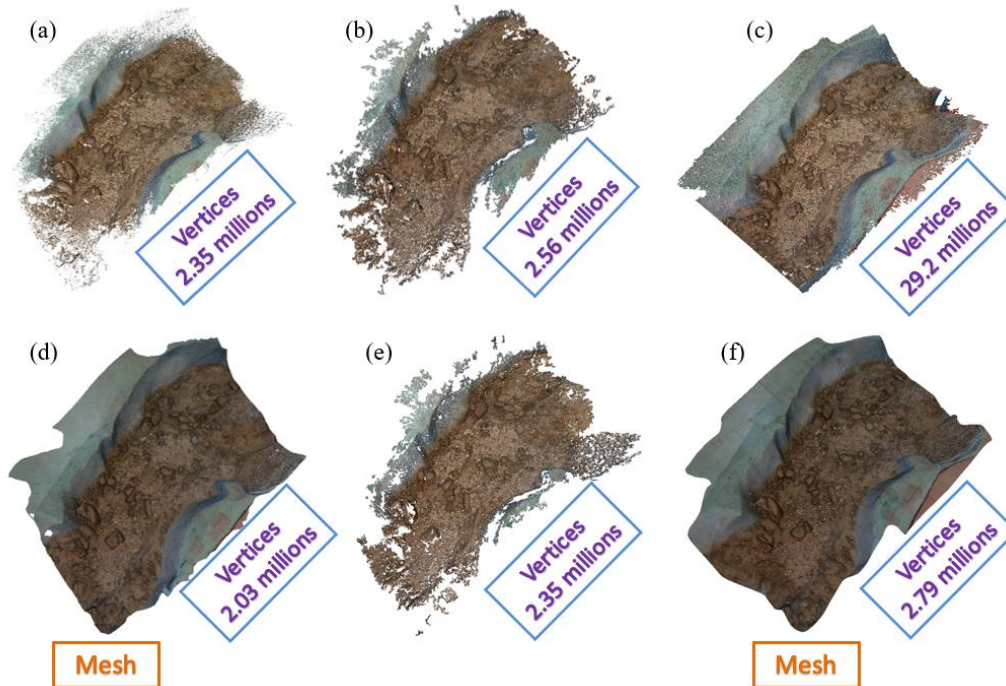

Figure 3. Outputs by (a) COLMAP, (b) Regard3d, (c) PhotoScan, (d) Meshroom, (e) VisualSfM and (f) ReCap and total number of vertices in respective outputs
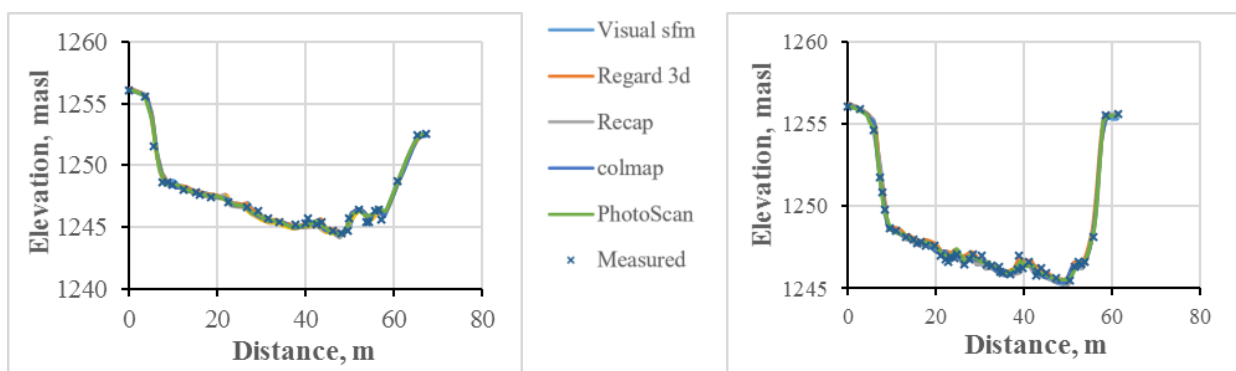

Figure 4. Cross section profiles (a) L9-R11 and (b) L9-R10

Table 2. Analysis of the error in predicting elevations by the selected software.

Tools	MAE	RMSE	R^2
Colmap	0.161 m	0.216 m	0.9958
Meshroom	0.176 m	0.232 m	0.9956
PhotoScan	0.155 m	0.195 m	0.9965
ReCap	0.165 m	0.222 m	0.9962
Regard3d	0.232 m	0.294 m	0.9946
VisualSfM	0.175 m	0.228 m	0.9956

5. *Conclusion*

From the results of this study, it can be said that SfM method can be used in hydraulic laboratories to efficiently capture 3D geometry from a physical hydraulic model in shorter time yet with better details and within acceptable accuracy. It is also concluded that the free and open source software are also capable of producing good results as compared to results from commercial software. Moreover, free and open sourced software offers more control to the users and hence have huge potential for researchers to produce even better-quality results. But for commercial purposes, where quality results are required in shorter time with minimum involvement of the user, commercial software are recommended. For example, PhotoScan and ReCap can perform all the processes including scaling of the final model output and DEM generation within one platform and hence provide the complete solution. Whereas, free and open sourced software requires additional third-party software to perform different processes e.g. Meshlab for geo-referencing the output model. Lastly, it should be noted that the first criterion to achieve better quality output is to take better quality photographs.

References

[1] Westoby M J, Brasington J, Glasser N F, Hambrey M J and Reynolds J M 2012 "Structure-from-Motion" photogrammetry: A low-cost, effective tool for geoscience applications *Geomorphology* **179** 300–14

[2] Snavely N, Seitz S M and Szeliski R 2008 Modeling the World from Internet Photo Collections *Int. J. Comput. Vis.* **80** 189–210

[3] James M R and Robson S 2012 Straightforward reconstruction of 3D surfaces and topography with a camera: Accuracy and geoscience application *J. Geophys. Res. Earth Surf.* **117**

[4] Micheletti N, Chandler J H and Lane S N 2015 Investigating the geomorphological potential of freely available and accessible structure-from-motion photogrammetry using a smartphone *Earth Surf. Process. Landf.* **40** 473–86

[5] Wu C 2013 Towards Linear-Time Incremental Structure from Motion *2013 International Conference on 3D Vision - 3DV 2013* 2013 International Conference on 3D Vision - 3DV 2013 pp 127–34

[6] Wu C VisualSFM: A Visual Structure from Motion System *http://ccwu.me/vsfm/*, 2011

[7] Wu C, Agarwal S, Curless B and Seitz S M 2011 Multicore bundle adjustment *CVPR 2011* CVPR 2011 pp 3057–64

[8] Schönberger J L and Frahm J 2016 Structure-from-Motion Revisited *2016 IEEE Conference on Computer Vision and Pattern Recognition (CVPR)* 2016 IEEE Conference on Computer Vision and Pattern Recognition (CVPR) pp 4104–13

[9] Cignoni P, Callieri M, Corsini M, Dellepiane M, Ganovelli F and Ranzuglia G 2008 *MeshLab: An Open-Source Mesh Processing Tool* (The Eurographics Association)

[10] Micheletti N, Chandler J H and Lane S N 2015 Structure from motion (SFM) photogrammetry

[11] Oniga V-E, Breaban A-I and Statescu F 2018 Determining the Optimum Number of Ground Control Points for Obtaining High Precision Results Based on UAS Images *Proceedings* **2** 352

[12] Goldstein E B, Oliver A R, deVries E, Moore L J and Jass T 2015 Ground control point requirements for structure-from-motion derived topography in low-slope coastal environments (PeerJ PrePrints)

[13] Alfredsen K, Haas C, Tuhtan J A and Zinke P 2018 Brief Communication: Mapping river ice using drones and structure from motion *The Cryosphere* **12** 627–33

Appendix 2: Image processing and Scaling steps in PhotoScan

1. *Processing of images with PhotoScan includes the following main steps:*

- Loading photos into PhotoScan
  1. Select Add Photos… command from the Workflow menu or click Add Photos toolbar button on the Workspace pane.
  2. In the Add Photos dialog box browse to the folder containing the images and select files to be processed. Then click Open button.
  3. Selected photos will appear on the workspace pane.
     Note: PhotoScan accepts JPEG, TIFF, DNG, PNG, OpenEXR, BMP, TARGA, PPM, PGM, SEQ, ARA (thermal images) and JPEG Multi-Picture Format (MPO). Any other format needs to be converted to above format.
- Inspecting loaded images, removing unnecessary images
  Images displayed in workspace can be visually inspected and unnecessary images can be removed by clicking cross (χ) sign.
- Aligning photos.
  1. Select Align Photos... command from the Workflow menu.
  2. In the Align Photos dialog box select the desired alignment options. Highest alignment of photos is recommended since it automatically rejects dark and less detail images and gives the best alignment resulting a good output. Click OK button when done.
  3. The progress dialog box will appear displaying the current processing status. To cancel processing click Cancel button.
- Building dense point cloud
  1. Check the reconstruction volume bounding box. To adjust the bounding box, use the Resize Region, Move Region and Rotate Region toolbar buttons. To resize the bounding box, drag corners of the box to the desired positions; to move- hold the box with the left mouse button.
  2. Select the Build Dense Cloud... command from the Workflow menu.
  3. In the Build Dense Cloud dialog box select the desired reconstruction parameters. Click OK button when done. Ultra-high and high dense cloud selection gave a very heavy point file. Around 96.7 million points for 116 images for high dense. This exported point cloud could not be loaded to other software like Meshlab and cloud compare neither in civil 3D and the software crashed. So, medium dense cloud selection is recommended. It gave a satisfactory output with considerable amount of point clouds around 8.7 million points for same number of images.
  4. The progress dialog box will appear displaying the current processing status. To cancel processing click Cancel button.
- building mesh (3D polygonal model)
  1. Select the Build Mesh... command from the Workflow menu.
  2. In the Build Mesh dialog box select the desired reconstruction parameters. Click OK button when done.
  3. The progress dialog box will appear displaying the current processing status. To cancel processing click Cancel button

- generating texture
  1. Select Build Texture... command from the Workflow menu.
  2. Select the desired texture generation parameters in the Build Texture dialog box. Click OK button when done.
  3. The progress dialog box will appear displaying the current processing status. To cancel processing click Cancel button.
- building digital elevation model
  1. Select the Build DEM... Command from the Workflow menu.
  2. In the Build DEM dialog box set Coordinate system for the DEM or choose the projection type.
  3. Select source data for DEM rasterization.
  4. Click OK button when done.
  5. The progress dialog box will appear displaying the current processing status. To cancel processing click Cancel button.
- Exporting results
  Before exporting the point cloud, it should be scaled (see2 Scaling for details)
  - Select Export Points... command from the File menu.
  - Browse the destination folder, choose the file type, and print in the file name. Click Save button.
  - In the Export Points dialog box select desired Type of point cloud - Sparse or Dense. Photo scan supports point cloud export of following types • Wavefront OBJ • Stanford PLY • XYZ text file format • ASPRS LAS • LAZ • ASTM E57 • ASCII PTS • Autodesk DXF • U3D • potree • Cesium 3D Tiles • Agisoft OC3 • Topcon CL3 • PDF.
  - Specify the coordinate system and indicate export parameters applicable to the selected file type, including the dense cloud classes to be saved.
  - Click OK button to start export.
  - The progress dialog box will appear displaying the current processing status. To cancel processing click Cancel button.

2. *Scaling*

PhotoScan supports setting a coordinate system based on either ground control point (marker) coordinates or camera coordinates. For both cases, the coordinates are specified in the Reference pane and can be either loaded from the external file or typed in manually.

In this study few reasonable ground control points (GCPs) were marked in the model before image acquisition. These GCPs were surveyed through theodolite and level machine with reference to pre-set benchmarks. The coordinates (XYZ) of the GCPs are saved in txt or csv file format with their respective names.

This file containing GCP coordinates can be imported to PhotoScan workspace.

- Click reference and click import, go to the folder containing GCP file and select the file and click open.
- In the import CSV dialog box select desired coordinate system. (In our case local coordinate system is selected. Then click OK.
- The reference marker points are then loaded in workspace.

- Placing markers

- Open the photo where the marker projection needs to be added by double clicking on the photos name.
- Switch to the marker editing mode using Edit Markers toolbar button.
- Zoom the photo and visually locate the marker point in photo, Right click at the point on the photo where the marker projection needs to be placed. From the context menu open Place Marker submenu and select the marker instance previously created. The marker projection will be added to the current photo.
- Repeat the previous step to place marker projections on other photos one by one.
- Place a marker in two images and PhotoScan will find the marker projections on the rest of the photos. If the projection of the marker is not satisfactory then it can be adjusted manually by lef clicking and dragging the marker to its desired position.
- After placing at least 4 markers, click update from reference menu to get a projection of all other markers with a scaled 3D product.
- Visually inspect the projection of markers in rest of the images and if necessary, manually drag the projection to its right location in the image. Then click update.
- Then we can get a 3D point cloud in absolute coordinate system, also we can see the marker projection in model tab in 3D.

Appendix 3: Detail layout of the physical 'model 1' of a reach of the river
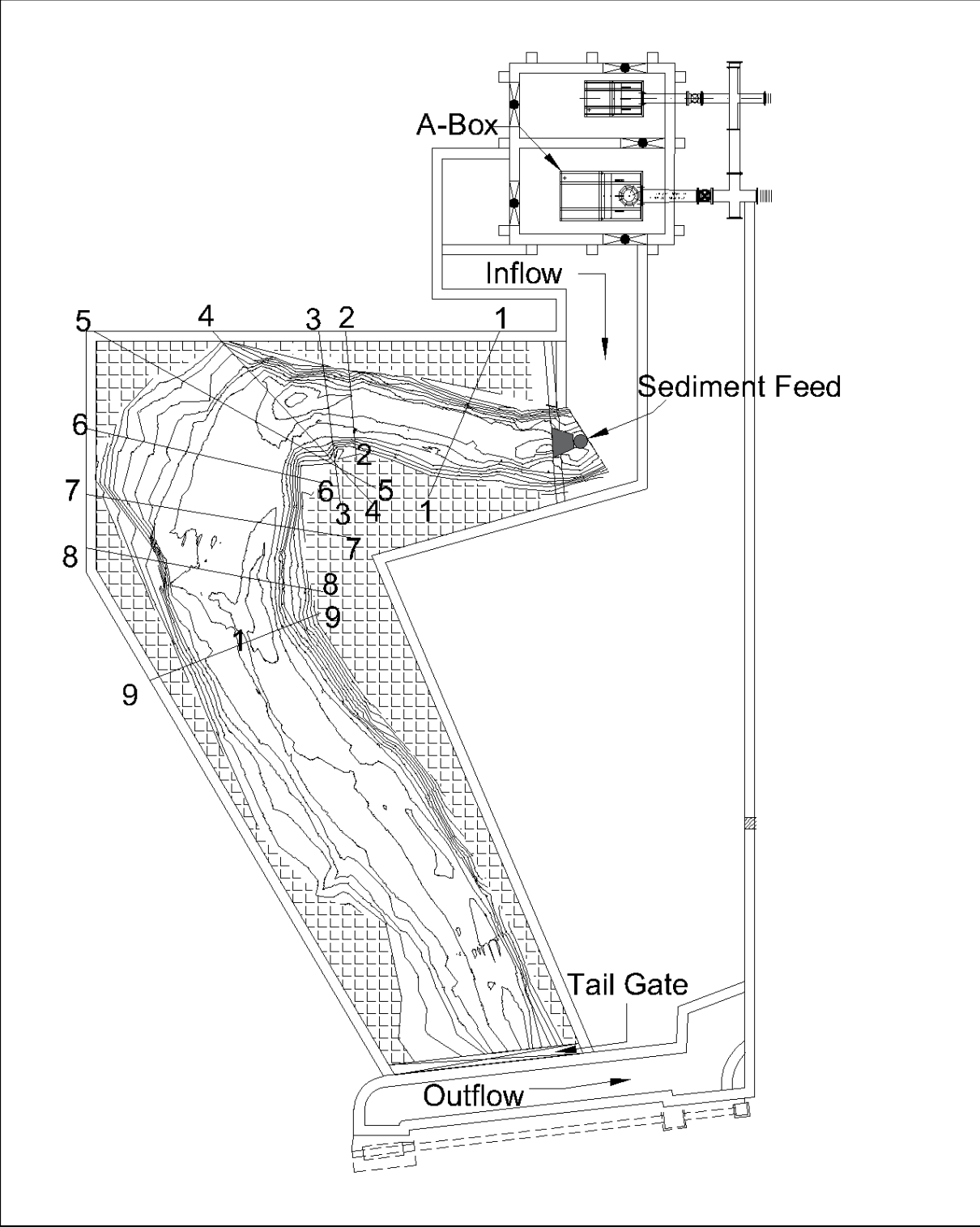
Appendix 4: Sample calculation for discharge and sediment transport feed rate

- **Discharge Calculation for Initiation of Motion**

Parameters	Symbol	Value	Units	
Average Width	B	1.40	m	
Slope	S	0.005		
Acceleration due to gravity	g	9.81	m/s2	
Temperature	T	20	oC	
Kinematic Viscosity	vs	1.01843E-06	m2/s	
Particle Size	D50	0.00055	m	0.55mm
Particle Size	D90	0.00128	m	1.28mm
Dimensionless Particle Size	D*	31.98691052		
Shields parameter		0.033608573		
Critical bed shear stress on the sediment particle		0.696326622	N/m2	
Hydraulic Radius	R	0.014196261	m	
Depth Required	h	0.014490127	m	1.45cm
Take Depth		0.024490127	m	2.45cm
Manning's Coefficient	n	0.017746749		
Wetted Area	A	0.034286177	m	
Hydraulic Radius	R	0.023662281	m	
Discharge Required For initiation of motion	Qc	0.004738953	m3/s	4.73895lps
Discharge Passed	Q	0.011259601	m3/s	11.25960lps
Velocity	V	0.328400591	m/s	
Bed Shear Stress	t	1.16063486	N/m2	
S	0.005			
B	1.4	m		
h	0.053132654	m	5.313265391	
n	0.0177			
A	0.074385715			
P	1.506265308			
R	0.049384205			
Q	40.00000028	lps		
Water Level in V-Notch	23.88037701	cm		
Scale Reading	32.76037701	cm		
Fall Velocity calculation				
Symbol	Julien (2002) - Check			
D	Value	Units		

G	0.0004	m	0.4	mm
vm	2.5			
g	1.02E-06	m2/s		
h	9.81	m/s2		
S	0.053132654	m	5.313265391	
u*	0.005			
shear velocity	0.051050531	m/s		
Settling Velocity	0.025525265	m/s	for the suspension criteria	
	0.054804907	m/s		
Meyer Peter -Muller (1948)				
D90				
D50	0.00128	m	1.28	mm
D10	0.00055	m	0.55	mm
Hydraulic Radius ®	0.00021	m	0.21	mm
Shear Velocity (u*)	0.049384205	m		
Dimensionless Critical Shield Stress Parameter(t*c)	0.051050531	m/s		
cb	0.047			
B	8			
t*o	1.5			
Dimensionless Sediment Transport Parameter(phi)	0.272089286			
Bedload discharge in dry volume per unit width of flume	0.854323246			
Feed Rate (kg/s)	4.43346E-05	m3/s/m		
	0.164481343	9.868880575	Kg/min	

Appendix 5: Sample calculation of GCP (X, Y) manually

Points	Horizontal Angle BM2 [Gradient]	Horizontal Angle BM2 [Degrees]	Angle BM2 to Y-Axis [Degrees]	Horizontal Angle BM4 [Gradient]	Horizontal Angle BM4 [Degrees]	X (m)	Y (m)
BM2	Counter Clockwise			Clockwise		563804.16	3082877.93
BM4						563363.38	3082784.67
LA	100.115	90.10	167.95	64.323	57.89	563954.47	3082173.76
L1	108.356	97.52	160.53	57.331	51.5979	564033.40	3082229.36
L2	116.806	105.13	152.93	49.433	44.49	564088.23	3082322.11
L3	122.548	110.29	147.76	44.222	39.80	564112.71	3082388.69
L4	118.700	106.8300	151.22	43.149	38.8341	564045.27	3082438.90
L5	109.812	98.83	159.22	42.370	38.13	563948.76	3082496.79
L6	87.024	78.32	179.73	46.996	42.30	563805.80	3082525.62
L7	67.925	61.13	196.92	59.796	53.82	563687.42	3082494.23
RA	113.580	102.22	155.83	57.828	52.05	564139.14	3082131.44
R1	107.634	96.87	161.18	62.785	56.51	564074.59	3082084.29
R2	118.479	106.63	151.42	53.283	47.95	564177.07	3082193.30
R3	130.428	117.39	140.67	43.588	39.23	564259.13	3082322.67
R4	141.307	127.18	130.88	35.176	31.66	564299.35	3082449.32
R5	149.631	134.67	123.39	27.030	24.33	564236.49	3082593.01
R6	152.815	137.53	120.52	21.696	19.53	564136.98	3082681.72
R7	145.881	131.29	126.76	19.744	17.77	564018.43	3082717.86
R8	106.744	96.07	161.98	20.926	18.83	563853.75	3082725.44
R9	57.129	51.42	206.64	26.370	23.73	563720.05	3082710.24
R10	35.493	31.94	226.11	38.991	35.0919	563601.43	3082682.91
BM1 to BM2	450.53	SQRT((G6-G5)^2+(H6-H5)^2)					
Absolute vertical angle	78.05	ABS(DEGREES(ATAN(((G6-G5)/(H6-H5)))))					
Bearing	258.05	IF(G6<G5,IF(H6>H5,(90-B27)+270,B27+180),IF(H6<H5,(90-B27)+90,B27))					
Calculation For LA							
X=	$G$5+($B$26/SIN(RADIANS(180-(C7)-(F7))))*SIN(RADIANS(F7))*(SIN(RADIANS(D7)))						
Y=	$H$5+($B$26/SIN(RADIANS(180-(C7)-(F7))))*SIN(RADIANS(F7))*(COS(RADIANS(D7)))						

Coordinate Calculation

Appendix 6: Sample calculation of GCP (Z) manually

Station 1					
SN	Station name	staff reading (m)	RL (Z) (m)	RL of BM1	275.000
1	BM1	1.118	275.000	RL of BM2	267.467
2	LA	1.25	285.560	RL of BM3	261.040
3	L1	1.134	276.280	RL of BM4	267.267
4	L2	1.243	285.000		
5	L3	1.144	277.080		
6	L4	1.131	276.040		
7	L5	1.18	279.960		
8	L6	1.157	278.120		
9	L7	1.259	286.280		
10	RA	1.264	286.680		
11	R1	1.226	283.640		
12	R2	1.195	281.160		
13	R3	1.235	284.360		
14	R4	1.082	272.120		
15	R5	1.06	270.360		
16	R6	1.098	273.400		
17	R7	1.207	282.120		
18	R8	1.156	278.040		
19	R9	1.059	270.280		
20	R10	1.074	271.480		

Appendix 7: Random manual distance measurement in model 1 and model 2
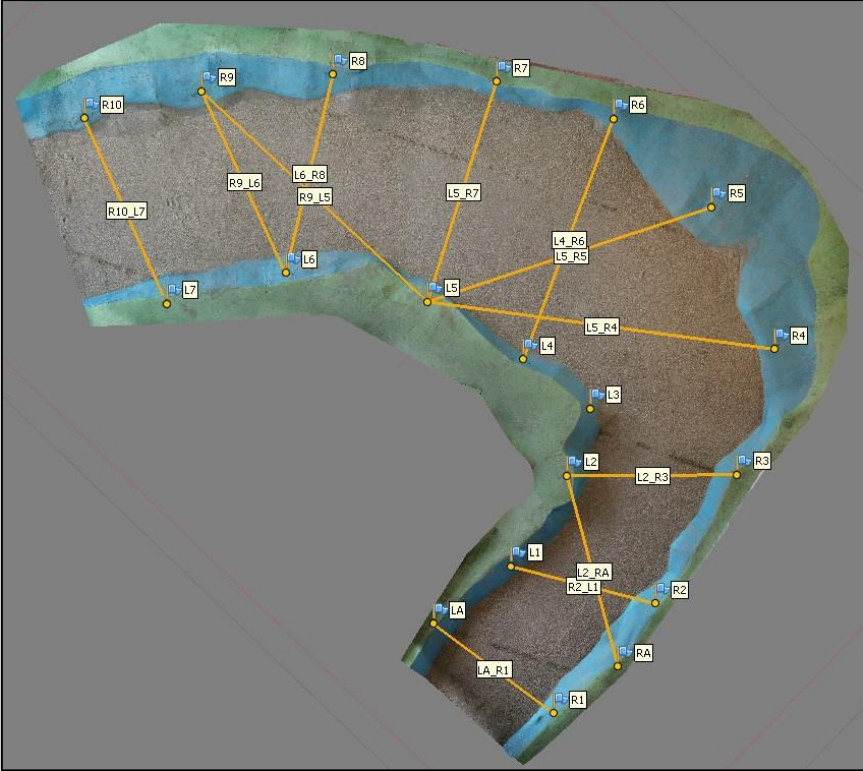

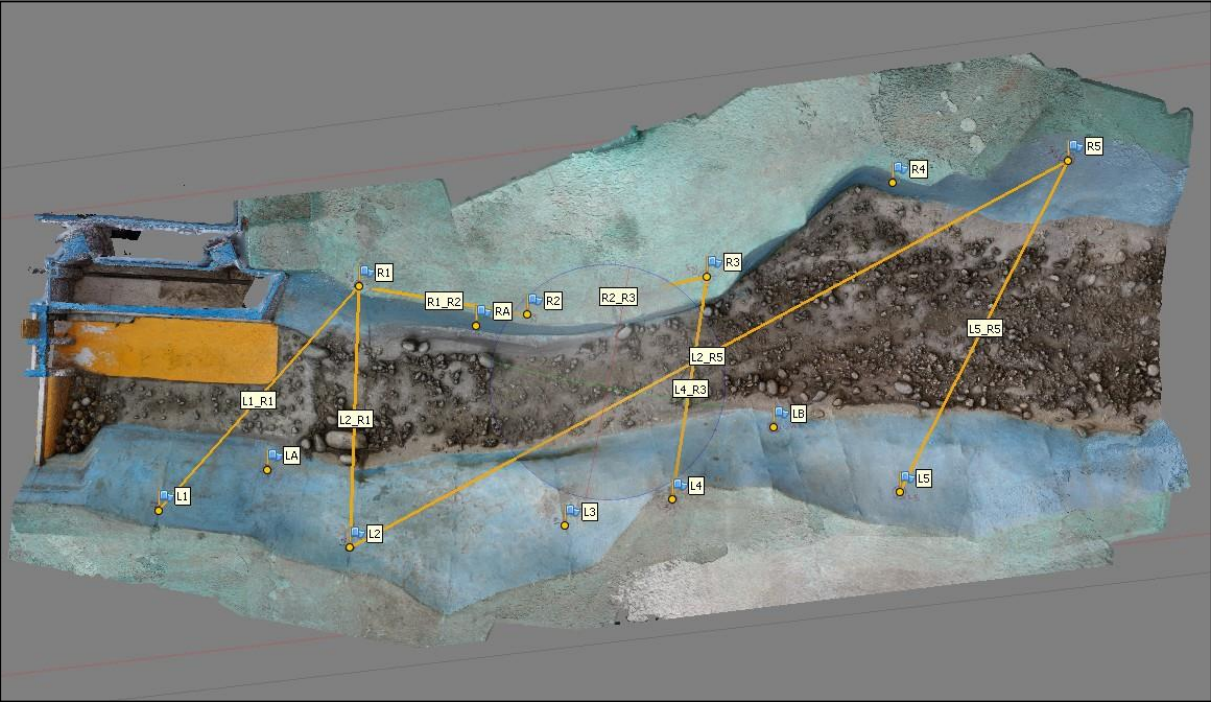
Figure A: Random manual distance measurement (Model 1)

Figure B: Random manual distance measurement (Model 2)